doi:10.20944/preprints202108.0231.v1

Article

Thermobarometry of Diamond Inclusions: Mantle Structure and Evolution Beneath Archean Cratons Worldwide

Igor Ashchepkov [1,*], Alla Logvinova [1], Zdislav Spetsius [2] and Hilary Downes [3]

[1] Institute of Geology and Mineralogy SD RAS, 630090 Novosibirsk, Russia; logv@igm.nsc.ru
[2] Alrosa Stock Company, 678174 Mirny, Russia; spetsius_zv@alrosa.ru
[3] Department of Earth and Planetary Sciences, Birkbeck College, University of London, London WC1E 7HX, UK; h.downes@ucl.ac.uk
* Correspondence: igor.ashchepkov@igm.nsc.ru; Tel.: +79505918327

Abstract: Thermobarometric calculations for mineral inclusions in diamonds provide a systematic comparison of PTXFO2 conditions for different cratons worldwide, using a database of 4440 mineral EPMA analyses. Beneath all cratons, the cold branch of the mantle geotherm (35-32 mWm^{-2}) relates to the sub-Ca garnets and rarely omphacitic diamond inclusions, referring to major continental growth events in Archean. High-temperature plume-related geotherms are common in Proterozoic kimberlites such as Premier, Mesozoic – Roberts Victor etc. and are common in Slave and Siberian cratons. In mobile belts: Limpopo, Magondi, Ural Ural, Khapchan belts and in the marginal parts of cratons like Kimberly Australia pyroxenitic and eclogitic pyroxenes and garnets prevail. The pyropes in the mobile belts are more Fe- and Ca-rich, in central parts of cratons, the peridotitic associations with sub- Ca pyropes prevail. The accretionary complexes like Khapchan and Magondi belts a thick eclogite-pyroxenite lens is highly diamondiferous.

Comparison by minerals shows that the PT estimates for clinopyroxenes and orthopyroxenes from peridotites and eclogites are representing mainly the middle part of the sub-lithospheric mantle while garnets gives more high-pressure estimates. refer to eclogites and reflect the processes of the differentiation during migration of partial melts. This produces the trends of joint decreasing Mg' and pressures. The PT for the chromites reflect conditions just above the lithosphere-asthenosphere boundary and mainly were formed due to interaction with the hydrous plume protokimberlite melts.

Archean diamond inclusions from Wawa province Canada are represented by Ca-enrich pyropes giving low-temperature conditions. Inclusions from younger kimberlites in Superior and Slave (and Siberian and East European) cratons show complex high-temperature geotherms due to plumes influence.

Peridotite garnets beneath the Amazonian craton indicate complex layering in the lithosphere base and a pyroxene layer in the middle part of SCLM. Diamond inclusions from the Kimberley craton of Australia show the greatest variations in the temperatures and composition.

Keywords: diamond inclusions; thermobarometry; pyrope; clinopyroxenes; chromite; eclogites; peridotites

1. Introduction

The sub-cratonic lithospheric mantle (SCLM) is the source of native diamonds as demonstrated by the rock associated with diamonds in kimberlites, and the typical mantle mineralogy of kimberlite diamond inclusions [1–8]. Diamond inclusions and associations (DIA) give direct information about the deepest accessible zones of the Earth. They can be used to decipher the ancient growth processes within the continental mantle, and the transformation of the cratonic mantle under the influence of melts and fluids related to deep mantle plumes and oceanic crustal subduction in ancient times.

 doi:10.20944/preprints202108.0231.v1

Diamond inclusions are divided into two major groups: peridotitic and eclogitic [8]. Peridotitic inclusions are more informative regarding their genesis and thermobarometry [9–11], but eclogitic inclusions can yield more information about the geodynamic conditions and history of the cratonic lithosphere [12–18].

Despite detailed studies of diamond inclusions, their association and their media of formation, and the major stages of their formation in Earth history [7,18–20], a systematic comparison of their thermobarometry have not been made because all together studies in previous only ~ 300 -400 gains and associations [8,20] were used on the diagrams and tables for direct PT estimates (excluding projections of temperatures on geotherm).

Many diamond inclusions were conservated in Archean time [18,19] and they provide very important information for the mantle composition and thermal stage of the mantle in early Earth stages.

It is very important to compare different cratons and their concrete parts to decipher the Early history of the Earth. The knowledge about the creation and composition of the deep parts of the mantle is still very restricted. It is necessary to provide the information and compare different constituting parts of the ancient continents and reconstruct the thermal regime of the ancient cratons. Nowadays there is no concrete information about the nucleation and further development of the cratons they are studying mainly using tectonics and geology of the Archean rocks on the surface, which were subjected to numerous modifications. Mantle rocks may give more information, but they were often also transformed. Diamonds are the containers that preserve the ancient materials from the deepest mantle zones from Archean time.

In this paper, we will use the set of consistent monomineral thermobarometers [21–28] to compare the conditions of diamond formation beneath different cratons worldwide and try to understand the reasons for the observed differences. Earlier review work [8] used a restricted set of minerals for thermobarometry used for peridotitic pyropes and clinopyroxenes. T. Stachel and J. Harris using a rather large database were mainly detailing the subdivisions to mineral types and gave a general outlook of their geochemistry. Here we are using a wider set of minerals and their compositions >4440 analyses (350 olivines) and give concrete information for many cratons mobile belts and their parts. We did not detail the difference between the parts of the Kaapvaal craton, dividing from others only Proterozoic Premier pipe. Also, the source rocks were not taken into account. The variations of the thermal regime in time were not systemized because the ages of diamond inclusions mostly do not know. More detailed work could be done after the receiving and accumulation of the new information.

2. Craton Settings of Kimberlites with Diamond Inclusions Worldwide

The studied mantle domains with diamond inclusions are represented on the worldwide scheme of [29] (Figure 1). This dataset is naturally incomplete but it includes >4440 published analyses collected from open sources mostly from dissertations (Table 1). We will show these data in some cratons, for example in the integrated diagrams, which may be quite different for different areas and pipes, depending on the location in separate terranes and mobile belts and on the time of kimberlite magmatism.

2.1. Siberian Craton

Previous studies [22–28] show that stratification beneath Yakutia and most cratons worldwide was formed by accretion of 6–7 plates of probable subduction genesis separated by pyroxenite, eclogite, metasomatic horizons and dunite lenses. The Siberian craton in Yakutia is a collage of microplates and tectonic terranes [30,31] (Figure 2) of different origins that were formed in the Early–Middle Archean [18]. Under the Anabar and Aldan shields, the mantle sections are more coarsely layered and consist of 3–4 large dunite horizons, separated by eclogite-pyroxenite lenses. Terranes that represent suture zones between protocratons, like Khapchansky located to the east of the Anabar shield, are often saturated with eclogites and pyroxenites at the mantle level. The pyroxenite layer at the

Preprints (www.preprints.org) | NOT PEER-REVIEWED | Posted: 10 August 2021 doi:10.20944/preprints202108.0231.v1

level of 3.5–4.5 GPa probably was formed in the Early Archean at high heat flux during the melting of eclogites [24,28].

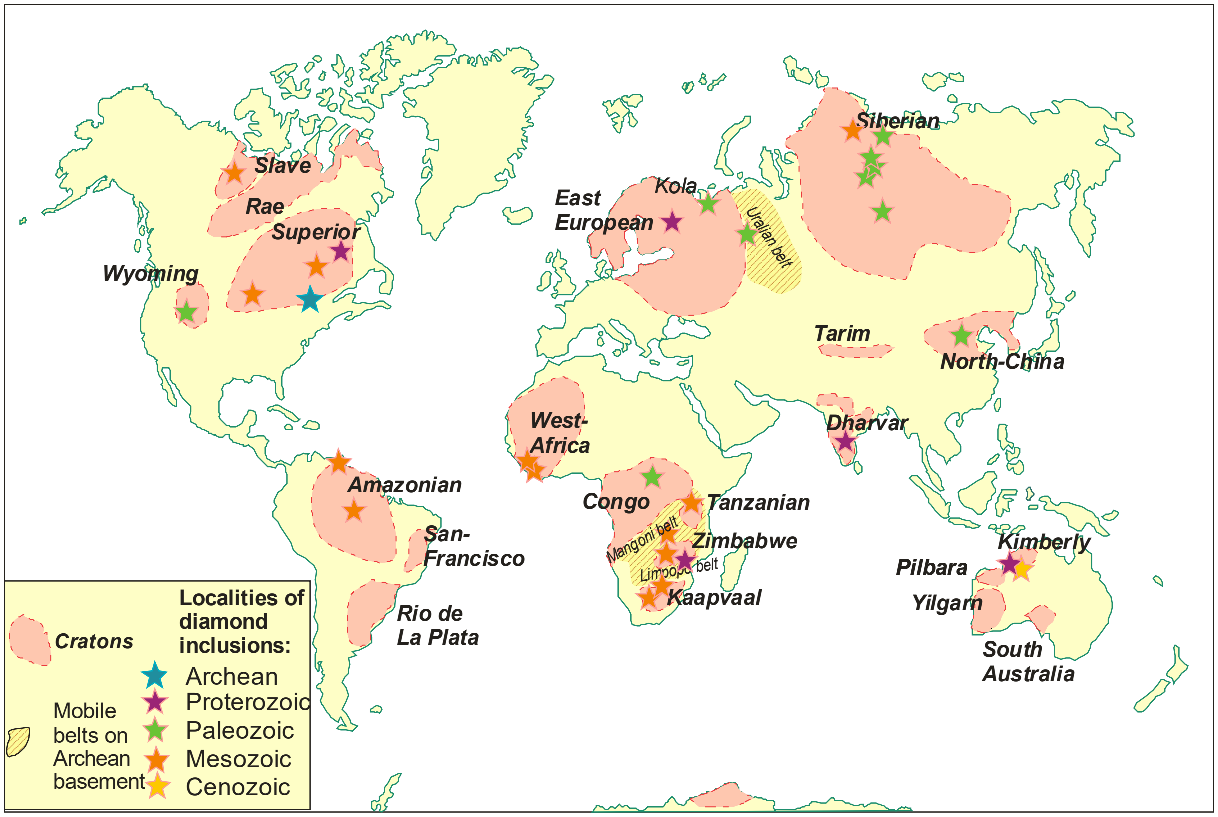

Figure 1. Location of the Precambrian cratons from [29]. The stars mark the location of the kimberlites with inclusions in diamonds for which were made PT estimates. The stars are marking the location of diamond inclusions. Blue star for Archean Wawa province, green stars for Proterozoic and Phanerozoic kimberlite provinces.

The Siberian craton was subjected to the kimberlite plume magmatism in Paleozoic and Mesozoic times crossing it from the north to south [32], and the mantle xenoliths and xenocrysts allow mantle reconstructions [24-28]. Within the early Archean protocratons, beneath granite-greenstone terranes such as Tungussky, Markhinsky, Berektinsky and Shary-Zhalgaysky, with an age of ~3.8–3.0 Ga [30,31], the mantle lithosphere is less depleted and often metasomatized. The Daldyn and Magan granulite-orthogneiss terranes have a layered SCLM structure [26] with folding shown in sections from North to South. From the Daldyn field to the Alakit field, the degree of metasomatism and alkalinity of pyroxenes and the amount of phlogopite are increasing and as well the number of chromites among the peridotites and diamond inclusions [33]. The most productive Aykhal and Yubileynaya pipes are confined to the dunite core, which is accompanied by changes of high field strength elements (HFSE) (Ta-Nb -Zr-Hf). Beneath the Magansky terrane, the thin-layered structure of the middle and upper part of the cratonic keel is replaced by a sharply depleted productive horizon at its base. The mantle beneath the granite-greenstone Markhinsky terrane contains different eclogites (including metapelitic type), suggesting subduction of the fragments of the continental lithosphere or pelitic sediments beneath the Khapchan terrane, the amount of eclogites in the lithospheric mantle exceeds the number of peridotites [34]. The diamonds and their inclusions are abundant also in the low stretches of the Lena River and the coast of the Laptev Sea but the compositions of DIA were not published.

Preprints (www.preprints.org) | NOT PEER-REVIEWED | Posted: 10 August 2021 doi:10.20944/preprints202108.0231.v1

2.2. Africa

Diamondiferous kimberlites were mainly found in the Kalahari supercraton consisting of the Kaapvaal and Zimbabwe cratons. Tanzanian, Congo and West Africa cratons also contain the diamondiferous kimberlites [35-38]. Congo and Tanzanian cratons and Limpopo, Magondi mobile belts have high importance in economic terms and definite interest from the scientific point of view. In Kaapvval craton the kimberlites trace the plume tails in different times: 1800–1700 Ma, 1110 Ma, 500–600 Ma, 110–130 Ma and 80-90 Ma [35,36]. Different groups of kimberlites have affinities varying from group II to group I in time [36]. Group-1 kimberlites have diverse ages. Cretaceous (Kimberley and Orapa), Permian (Jwaneng), Cambrian (Venetia) and Proterozoic (Premier-Cullinan). Details of ages and references are possible to find in reviewing works [35-37].

All kimberlites have different rather high diamond grades [37]. The most abundant are in Premier (Cullinan) pipe where they have a high-temperature signature and huge diamonds due to plume influence [38]. Mesozoic kimberlites commonly have varied in their diamond grade and sizes and properties and morphology diamonds having different ages.

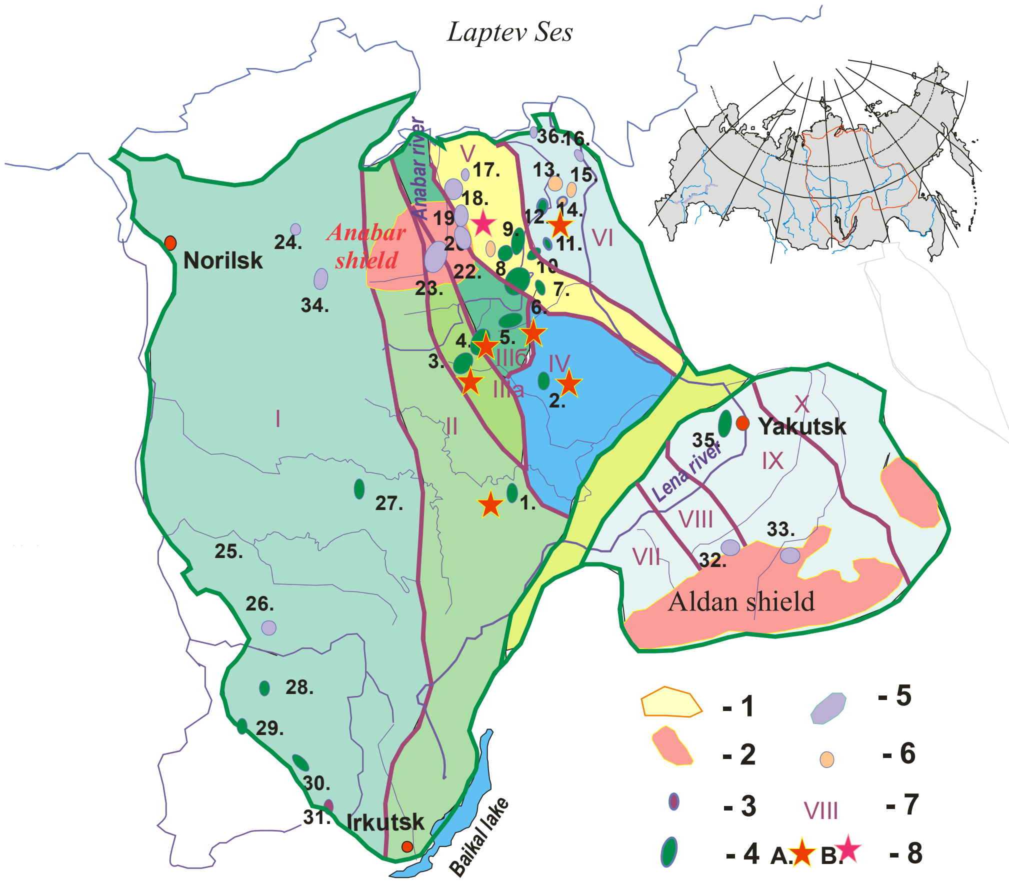

Figure 2. Location of kimberlite and kimberlite fields on the Siberian platform [32]. 1. Malo-Botuobinsky, 2. Nakyn; 3. Alakit-Markha, 4. Daldyn, 5.Upper Muna, 6. Chomurdakh, 7. Severnei, 8. West Ukukit, 9. East Ukukit, 10. Ust-Seligir, 11.Upper Motorchun, 12. Merchimden, 13. Kuoyka, 14. Upper Molodo, 15. Toluop, 16. Orto-Yargyn, 17. Ebelyakh, 18. Staraya Rechka, 19. Ary-Mastakh, 20. Dyuken, 21. Luchakan, 22. Kuranakh, 23. Middle Koupnamka, 24. Middle Kotui, 25. Chadobets, 26. Taichikun-Nemba, 27. Tychan, 28. Muro-Kova, 29. Tumanshet, 30. Belaya Zima, 31.Ingashi, 32. Chompolo, 33. Tobuk-Khatystyr, 34. Kharamai. 35. Manchary; 36. Karny sediments. I. Siberian platform. II. Shields. III. Precambrian kimberlites. IV. Palaeozoic kimberlites. V. The Triassic kimberlites. VI. kimberlites of the upper Jurassic. VII. Tectonic terranes according to [31]. VIII. Location of the studied fields with the diamond inclusions. A. In Devonian kimberlites. B. Ebelyakh diamond placer.

2.3. North America

In Canada, the oldest diamonds were found in the Archean Ca-alkaline lamprophyres (2.7Ba) in the Wawa district Ontario Superior craton. The other localities in Superior include the Renard kimberlites in Quebec with an age of 654–656 Ma [36,39,40] and the Attawapiskat kimberlites of age ~187–183 Ma [42] and Fort la Corne about 100 Ma [43].

In the Slave craton, the older kimberlites of Snap Lake are 537 Ma old [44], whereas the well-known Jericho kimberlite (173 Ma) and Lac de Gras kimberlites are Mesozoic.

In the Wyoming craton of Montana, kimberlites from the Front Range [45] diamonds are found in Devonian Sloan and Kelsey Lake pipes but the diamond inclusions are different as well as the structure of the mantle columns [46].

2.4. South America

In South America diamonds are found mainly in placers in the Amazonian craton and very few kimberlites contain diamonds. The kimberlites in Venezuela (Guyana shield) have Neoproterozoic age [47,48]. In the Central Brazilian shield of the Amazonian craton in Juina, the known kimberlites with diamonds are dated ca. 70–80 Ma [49,50].

In the Sao Francisco craton, the known kimberlites have Neoproterozoic ages [51] but most kimberlites occur in off craton settings [52] and are common of low diamond grade.

Table 1. The location of the sources of diamond inclusions and the bibliographic sources.

Region	Craton	Area	Eclogite DIA %	Pipe	Reference
North America	Superior	Wawa	27%	Lamprophyre dyke	[53–56]
	Superior	Quebec	32%	Renards	39,40]
	Superior	Attawapiskat		T1 and U2	[42,57,58]
	Superior	Alberta, Buffalo Head Hills		K11, K91 and K252	[59]
	Slave	Snap Lake	29%	Snap Lake	[60–64]
	Slave	Northern Slave, Muskox		Jericho	[16,65–69]
	Slave	Lac de Gras		DO27, A154, A21, A418, DO18, DD17 and Ranch Lake	[70–73]
	Wyoming	Front Range	48%	Kelsey Lake	[74]
	Wyoming	Front Range		Sloan	[75]
South America	Amazonian	Brazil	44%	Juina	[76–78]
	Amazonian	Venezuela			[47,48]
	Sao Paulo	Brazil		Fazenda Largo	[49]
Africa	Kaapvaal	South Africa, Mz	47%	Jagersfontein	[79,80]
	Kaapvaal	South Africa		Koffiefontein	[80,81]
	Kaapvaal	South Africa		Rietfontein	[82]
	Kaapvaal	South Africa		Finsch	[83–88]
	Kaapvaal	South Africa		Bultfontein	[89]
	Kaapvaal	South Africa		Roberts Victor	[91–95]
	Kaapvaal	South Africa		De Beers Pool	[83, 90]
	Kaapvaal	South Africa		Voorspoed	[96]
	Kaapvaal	South Africa		Lace	[97,98]
	Kaapvaal	Swaziland		Dokolwayo	[99]
	Kaapvaal	South Africa		Monastery	[100]
	Kaapvaal	Botswana		Jwaneng	[105,109–110]
	Kaapvaal	Lesotho		Letseng -la-Terai	[103]
	Kaapvaal	South Africa, Pz	45%	Premier	[38,84,86,87,101,102]
	Magondi belt	Botswana	44%	Damtshaa	[106,107]
	Magondi belt	Botswana		Letlhakane	[107,108]
	Magondi belt	Botswana		Orapa	[15,104-108]
	Limpopo belt	Zimbabwe	47%	Venetia	[112–114]
	Limpopo belt	Zimbabwe		River Ranch	[115]
	Tanzanian	Tanzania	32%	Murowa	[116]
	West African	Man shield	40%	Koidu	[117]
	West African	Man shield		Akwatia	[5]
	West African	Man shield		Ghana	[118]
	West African	Man shield		Kankan	[119]
	Congo	Kasai craton	64%	Alluvial placer	[120]

Preprints (www.preprints.org) | NOT PEER-REVIEWED | Posted: 10 August 2021 doi:10.20944/preprints202108.0231.v1

	Congo	NE Congo		Catoca	[121]
Australia	Kimberly	N Australia	69%	Ellendale	[122]
	Kimberly	N Australia		Argyle, Ellendale	[123–127]
Siberia	Siberian	M.Botuobinsky	14%	Sputnik	[128]
	Siberian	M.Botuobinsky		Mir	[17,32,129–132]
	Siberian	M.Botuobinsky, Daldyn, Alakit		Mir, Udachnaya, Internatsionalnaya, Aykhal, Sytykanskaya, Yubileynaya, Komsomolskaya and Krasnopresnenskaya	[133-137]
	Siberian	Daldyn	64%	Udachnaya	[2,137–140]
	Siberian	Daldyn		Dalnyaya, Zarnitsa	[141]
	Siberian	Alakit	15%	Sytykanskaya	[142]
	Siberian	Alakit		Yubileinaya, Komsomolskaya	[133–137]
	Siberian	Alakit		Komsomolskaya, Krasnopresnenskaya	[138]
	Siberian	Alakit		Komsomolskaya	{143]
	Siberian	Alakit		Aykhal	[134]
	Siberian	Nakyn	91%	Nyurbinskya	[145–148]
	Siberian	Ebelyakh	92%	Mayat, Kholomolokh	[34]
East Europe	East European	Arkhangelsk	44%	Arkhangelsk	[148–150]
	East European	Finland		Lahtojoki	[151]
	East European	Urals	83%	Urals placers	[152–154]
China	Sino-Korea craton	China, Mengyin	0%	Shengli, pipe 50	[155]
Kalimantan	Borneo	Kalimantan	10%	placers	[156]

2.5. Australia

Known kimberlites in Australia are of low diamond grade or barren. Diamonds and their inclusions were investigated in the margins of Kimberly craton. Argyle lamproite pipe [122–127] is situated within the Creek Mobile Zone and Ellendale within the Leopold Mobile zone). They have quite different ages, 1126 Ma and 20.6 Ma respectively.

2.6. East-European Craton

There are several localities of diamonds in East European craton. The Arkhangelsk Devonian kimberlites in NE part [148–149]. Vendian and late Proterozoic kimberlites contain diamond-bearing xenoliths and diamonds also. In Devonian Priazovie kimberlites, diamonds are extremely rare. In Finland, the Lahtojoki pipe contain diamonds [151]

2.7. Ural Mobile Belt

In the western slope of Urals diamond-bearing tuffites and placers of diamonds with the inclusions were discovered. Inclusions reveal Devonian ages and mainly are of eclogitic affinity [152–154].

2.8. North China craton

In China, the diamonds and hosting kimberlites were discovered mainly within the North China (Sino-Korean) craton. The main deposits are located in the Mengyin kimberlite field (Shandong province) which contain also diamonds with inclusions [155].

2.9. Malaysia

The placers in Kalimantan contain beautiful diamonds with diamond inclusion [156]. They are related to the kimberlites because the picroilmenite nodules are associated with the diamonds.

India was for a long time the most productive region for diamonds but discovered inclusions in lamproites are represented by olivines only [157] which does not allow the thermobarometric estimates without the precise measurements.

3. Thermobarometric Methods

A major problem of interpretation of the location of diamonds in the SCLM is thermobarometry. For Cr-diopside, the single grain barometer of P. Nimis and W.Taylor [158] gives rather good estimates [159,160] but does not work for the low-Cr eclogitic and basaltic pyroxenitic systems. S. Simakov and L.Taylor [161] suggested a barometer using a series of equations and references which gave estimates for eclogitic Cpx but without direct formulae, so it is difficult for other people to use this thermobarometer. The garnet thermobarometer of C. Ryan [162] uses the Ni-thermometer for peridotitic garnets [10,163] and an empirical garnet barometer using Cr in garnet to determine the Al in coexisting pyropes and then the Al-in-Opx barometer after D.McGregor [164]. This procedure gives appropriate results only for very depleted sub-Ca garnets [165]. Another method of PT estimates was obtained by the projection of the Ni-in-garnet temperatures to previously obtained geotherm or a common 40 mWm^{-2} geotherm [162]. The attempt to use this method for the diamond inclusions [8] produce the appropriate results for <10% only and some part of them are locating outside the diamond stability field [166,167]. Usage of the Cr- tchermakite [158] gives results only for about 103 of Cpx from the al data base. Mostly they reveal pressure below 3 GPa and they demonstrate quite variable thermal conditions (SF1, Fig.1), major part is tracing relatively low-temperature. There is also to use the Ca-Cr content in garnets for the pressure estimates by [165] but it can be used for numeric results. The application of the Opx [168] thermometer together with Opx barometer [164] using an iteration scheme in the PT program gives appropriate results for 290 analyses from all data (SF1, Fig.2). This method produces very similar results to those obtained by the Gar-Opx barometry [168,169].

We used the system of the published thermobarometers for the major peridotitic minerals developed by I.Ashchepkov: clinopyroxenes (Cpx), orthopyroxenes (Opx), garnets (Gar), chromites (Chr), ilmenites (Ilm) [21–28]. For the Cpx in the peridotitic system, a Jd-Di barometer [21,22,24] is used. In combination with the modified Cpx thermometer [158] it produces the wider PT plot for 150 peridotitic clinopyroxenes (SF1, Fig.3).

The corrected Jadeite-Diopside Cpx barometry is used also for the omphacites in the eclogitic system [24] (SF1, Fig.4). It produces a rather dense plot in the middle part of the mantle-3-4.5 GPa (SF1, Fig.4).

The modified Cr- garnet barometer [24] together with the monomineral version of Gar-Ol thermometer [170] applicated for the pyrope garnets. Most of the PT estimates trace the LT -35mWm-2 geotherm.

The eclogite garnet barometer in combination with the Gar-Cpx thermometer [171] gives appropriate results for the Ca-, Na-bearing garnets using the dependence of Na in garnet from pressure with FeO varying from 12 to 30 wt.% [24]. For the Cr-spinels and chromites, we calibrated their dependence of Cr# on pressure separately in garnet and spinel mantle facies [21]. The barometer is in combination with the spinel-olivine thermometer of [172] where the Fe#Ol is calculated from Fe#Ilm and T °C by the empirical equations.

Although ilmenite inclusions are rare in diamonds (17), and sometimes occur in diamond-bearing xenolith [140] we successfully used the dependence geikelite mineral ($MgTiO_3$) [27] from pressure for barometry in combination with the ilmenite-olivine thermometer [172] where the Fe#Ol is calculated from Fe#Ilm and T °C by the empirical equations.

The precision of the used thermobarometric methods was shown in the previous publication [24

It is close to 0.2–0.1 GPa for Cpx –Gar- Chr method for peridotites and to 0.4–0.5 for eclogites. The pressure estimates for almandine barometer are highly sensitive to the precision of Na analyses.]. The correlations of the estimates with the J-Di barometer is high (see SF1, fig.8). As well the calibration using the experimental data is quite good for all methods [24], (SP1, Fig.9).

Preprints (www.preprints.org) | NOT PEER-REVIEWED | Posted: 10 August 2021 doi:10.20944/preprints202108.0231.v1

For the calculation of the oxygen fugacity the monomineral version of the G.Gudmundsson, B.Wood [174] for peridotitic garnets. The Fe3+ is determined by the stoichiometry. Since the method of the V. Stagno [175] for eclogites needs also the Fe3+ clinopyroxenes we skipped the FO2 estimates for eclogitic garnets. The FO2 for ilmenites and chromites according to [172] in monomineral version, for ortho- and clinopyroxenes, the polynomial formulas [23] were used.

All these thermobarometers are combined in the PT program Ter55 written in FORTRAN-70 [25].

4. Results of Thermobarometric Reconstructions for Diamond Inclusions

4.1. Results of Thermobarometry of Mineral Inclusions in Diamonds of Yakutia.

For diamond inclusions from Siberian kimberlite pipes, regularities were determined using data from the following authors: [126–145] and others. We used the total set of 2145 analyses for the construction of the PTX diagrams for individual areas of kimberlite magmatism. Preliminary information about the structure of the lithosphere was published in series of papers [21–28].

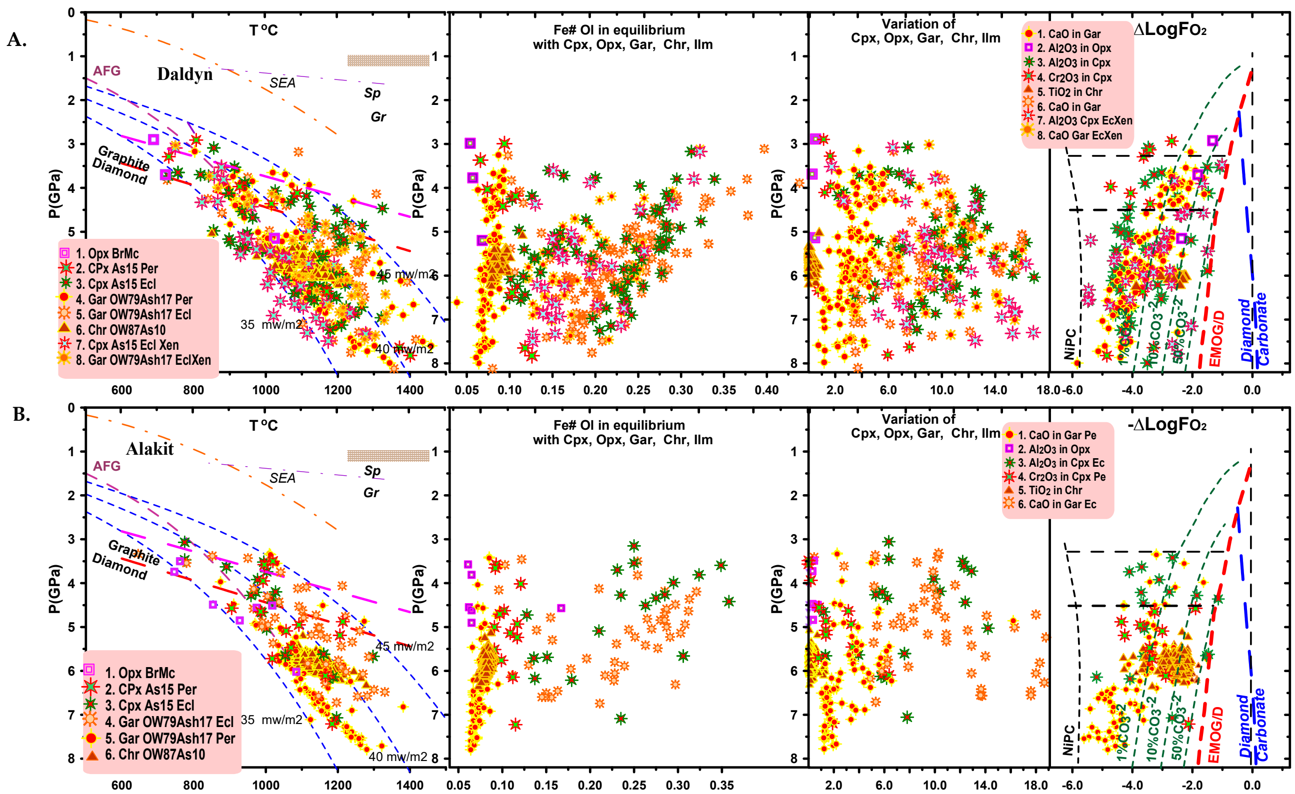

Figure 3. PTXFO2 diagram for diamond inclusions from (**A**) Daldyn kimberlite field; (**B**) Alakit kimberlite field. Yakutia. **Signs.** Opx: T°C [165]–P (GPa) [161]; Cpx: 2. T°C [156]–P (GPa)[24] for diamond inclusions from peridotites; 3. The same for eclogitic DIA; 4. Garnet (monomineral): T°C [167]–P (GPa) [24] for diamond inclusions fromeclogites; 5. T°C [168]–P (GPa) [24] for peridotitic garnets. 6. Chromite for diamond inclusions: T°C [167]–P (GPa [24]); 7. T°C [156]–P (GPa)[24] Cpx from eclogite xenolith. 8. T°C [167]–P (GPa) [24] Gar from eclogite xenolith. Position of conductive geotherms are after [176] and the graphite—diamond transition after [158]; the same line above after [159]. SEA South-East Australian geotherm [177]. AEG - The geotherm for mantle xenolith from Archangelsk mantle [171]. The lines EMOG/D [178] and Diamond/Carbonate [175] buffersand concentration of $\%CO_3^{2-}$ in melts [179] in diagram P-FO2. NiPC-nickel precipitation curve [173]. AFG – Arkhaneklsk geotherm [180]. Data for diamond eclogite associations from Udachnaya [181-187].

Preprints (www.preprints.org) | NOT PEER-REVIEWED | Posted: 10 August 2021 doi:10.20944/preprints202108.0231.v1

4.1.1. Daldyn Field

Pyrope garnet diamond inclusion of the Daldyn field are from diamonds from Udachnaya pipe [2,137-140] and several grains from Dalnyaya and Zarnitsa [141] pipes (Table 1). The PT array for garnet inclusions is divided into two groups near 5 GPa. They formed the joint array of increasing Fe# with decreasing pressures (IFDP), but they differ in CaO. Variations in CaO are quite wide and the most depleted garnets belong to the depth interval >6.5 GPa. There is an increase and splitting of the P- CaO trends with decreasing pressure. Eclogite clinopyroxenes and garnets show two IFDP trends of increase of iron content from Fe#Ol ~10–15 to 16–37 wt.% with a decrease in pressure from 7.5 to 3.5 GPa. The latter nearly coincides with the garnet IFDP trend. The decrease in Fe in pyroxenes is found at 7–7.5 GPa. The most CaO-rich garnets and Al_2O_3 clinopyroxenes are found at 5–6 GPa. Clinopyroxene differences are less dependent on the estimated depth. (Figure 3A). The chromite IFDP trend is nearly coinciding with the Cr-pyrope trend in 6.2-5 GPa interval being slightly higher in Fe#.

The trend for the eclogitic garnets splits into two trends in the PT plot (Figure 3A). The low-temperature (LT) branch coincides with the LT branch of pyrope garnets. The others form a rather scattered plot between the 45 and 35 mWm^{-2} geotherms. The chromites plot on the dense cluster together with the high population of the eclogitic garnets just at the inflexion of the convective branch usually traced by the deformed or sheared peridotites [4]. Many eclogitic and pyroxenitic varieties plot in the high-temperature (HT) field and coincide with the diamond-graphite boundary [166,167]. The clot of the point with the boundary at 3.4-4.5 GPa corresponds to the middle pyroxenite layer [187].

In the P-fO_2 diagram, the eclogitic CPx and Cr-rich garnets form the less oxidized branches ~−5 relative to ΔQMF (Quartz-Magnetite-Fayalite buffer) [171] and this is a common trend for African [and other cratons worldwide 188]. At lower pressure, they form the inclined trend. The diamond stability boundary for peridotitic [178, 179] and eclogitic associations [175] does not completely coincide. The peridotitic clinopyroxenes, eclogitic garnets and chromites are essentially more oxidized to −1 ΔQMF [175].

4.1.2. Alakit Field

Among the Alakit diamond inclusions (Table 1), sub-calcic dunitic pyropes dominate over eclogitic garnets. The Cr-rich garnets reveal nearly the same trend of IFDP in the P-Fe# plot as those from Daldyn but more Cr-rich varieties strongly prevail. Varieties of Cr garnets with 4 and 6 wt% CaO are found at a greater lower depth than more depleted varieties. They reveal two separate branches at pressures <6 GPa. The chromite trend is nearly the same in large diamondiferous pipes and the number of chromites in diamond inclusions and associations everywhere prevail over the garnets. Eclogite pyroxenes and garnets (Table 1) form a similar upward IFDP trend as in the Daldyn field but with a steeper increase of iron and the Fe-rich part is mainly composed of garnets. The low-Cr Mg-rich pyroxenes are confined mainly to the average pressure range as well as for enstatites which belong to the 5.0–3.5 GPa interval and mainly form the pyroxenite layer. The proportion of chromites is much higher compared to Daldyn diamonds (Figure 3B). The pyropes in the high pressure are oxidized less than −4 ΔQMF. The values for chromites vary from −2 to −4. Eclogitic garnets are less oxidized and are close to EMOG/D buffer [163] but omphacites are relatively reduced.

4.1.3. Malo—Botuobinsky Field

In the PT plot for the Mirninsky (Malo-Botuobinsky) region [128–132], the DIA pyropes have an opposite trend, i.e., the largest variations in CaO are in the lower part of the section and the most magnesian dunite varieties form an interval from 6.5 to 5 GPa, and then above them, the harzburgitic garnets again appear in the middle of the SCLM. There is a high proportion of peridotite Cr-bearing varieties of ortho-and clinopyroxenes in the middle part of the mantle column, which suggests that the pyroxenites originated from the peridotite partial melts. This more enriched horizon possibly is complementary to the

Preprints (www.preprints.org) | NOT PEER-REVIEWED | Posted: 10 August 2021 doi:10.20944/preprints202108.0231.v1

depleted lower SCLM. Omphacites together with garnets form an IFDP in the PT P-Fe# plot (Figure 4A).

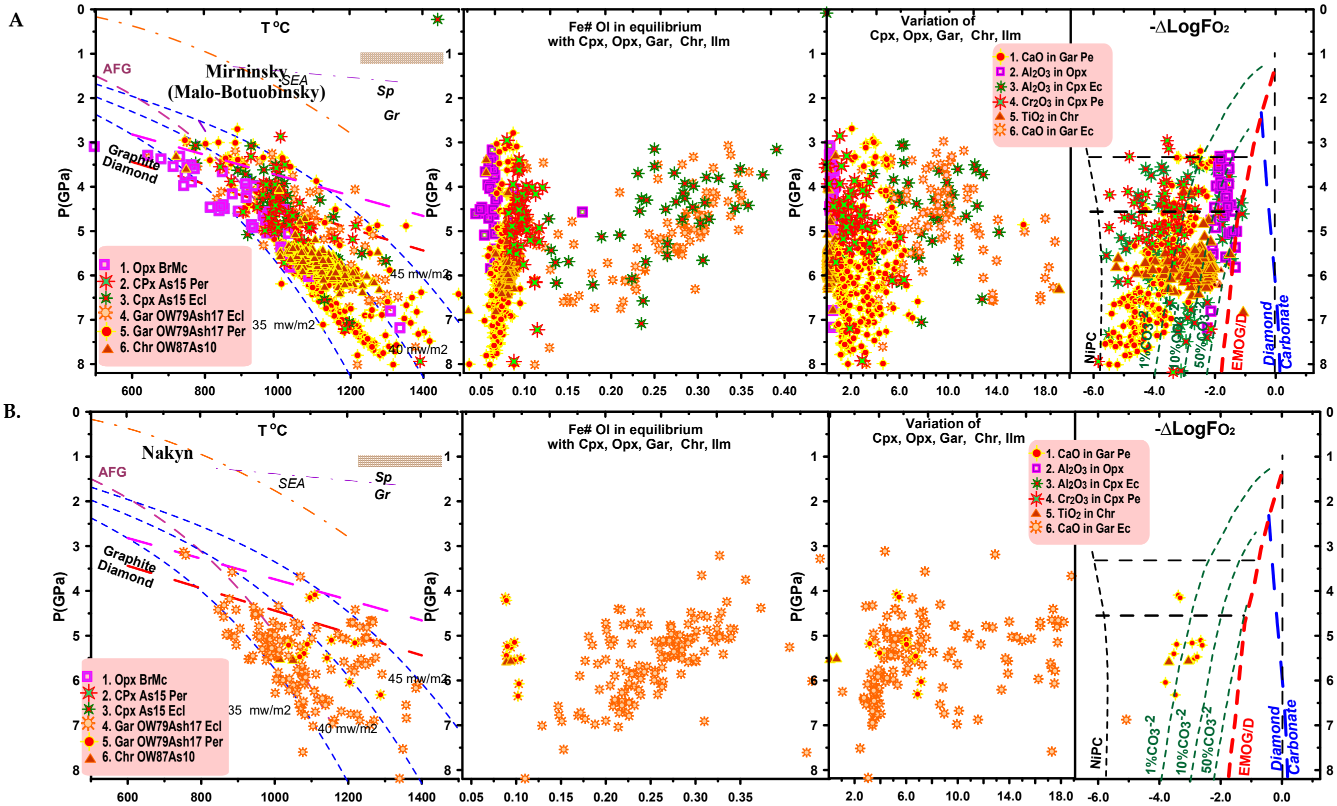

Figure 4. PTXFO2 diagram for diamond inclusions from (**A**) Mirninsky field; (**B**) Nakyn kimberlite field Yakutia. Symbols are the same as in Figure 3.

The geothermal conditions traced by diamond inclusions also refer to two branches. Even Cr-garnets partly trace the convective branch is not so evident in the middle part. The Cr garnets are found also at more HT conditions at the deeper part of the SCLM. But most of them are plotting within the 35–40 mWm^{-2} geothermal interval. The Cr-pyroxenites and Cr-diopsides form the colder branches—to 35 mWm^{-2} geotherms or even lower. In the P-fO$_2$ diagram, the less oxidized conditions correspond to the eclogitic clinopyroxenes in the middle SCLM. At high pressures, the lowest in fO$_2$ conditions corresponds to the Cr-rich garnets.

4.1.4. Nakyn Field

In the Nakyn field [145–147] all pipes are very rich in eclogitic material and Al-rich Cpxs prevail in the mantle peridotites and eclogites (Table 1). Cr-pyropes are relatively rare and belong to the lherzolite harzburgite type and the latter is even more rarely found. Among inclusions, almandines dominate, which also form a broad uptrend of P-Fe#. They formed the dispersed IFDP trend. The Fe-poor garnets yield deeper conditions. Two horizons with the Ca-rich associations going to grospydites are found at 6 GPa and in 6–7 GPa intervals. The Fe-enriched varieties are rare and refer to the MSCLM (Figure 4B).

The geotherm formed by the eclogitic garnet varies from 33-37 mWm^{-2} (most of the garnets) to 45 mWm^{-2}. The separate clots trace the diamond-graphite boundary in various heating degrees. Practically all Cr-garnets show HT temperature conditions, some of them trace the convective branch and the others yield even more heated conditions. And this may explain the hybridism of the eclogitic and peridotitic material in SCLM.

A.

B.

C.

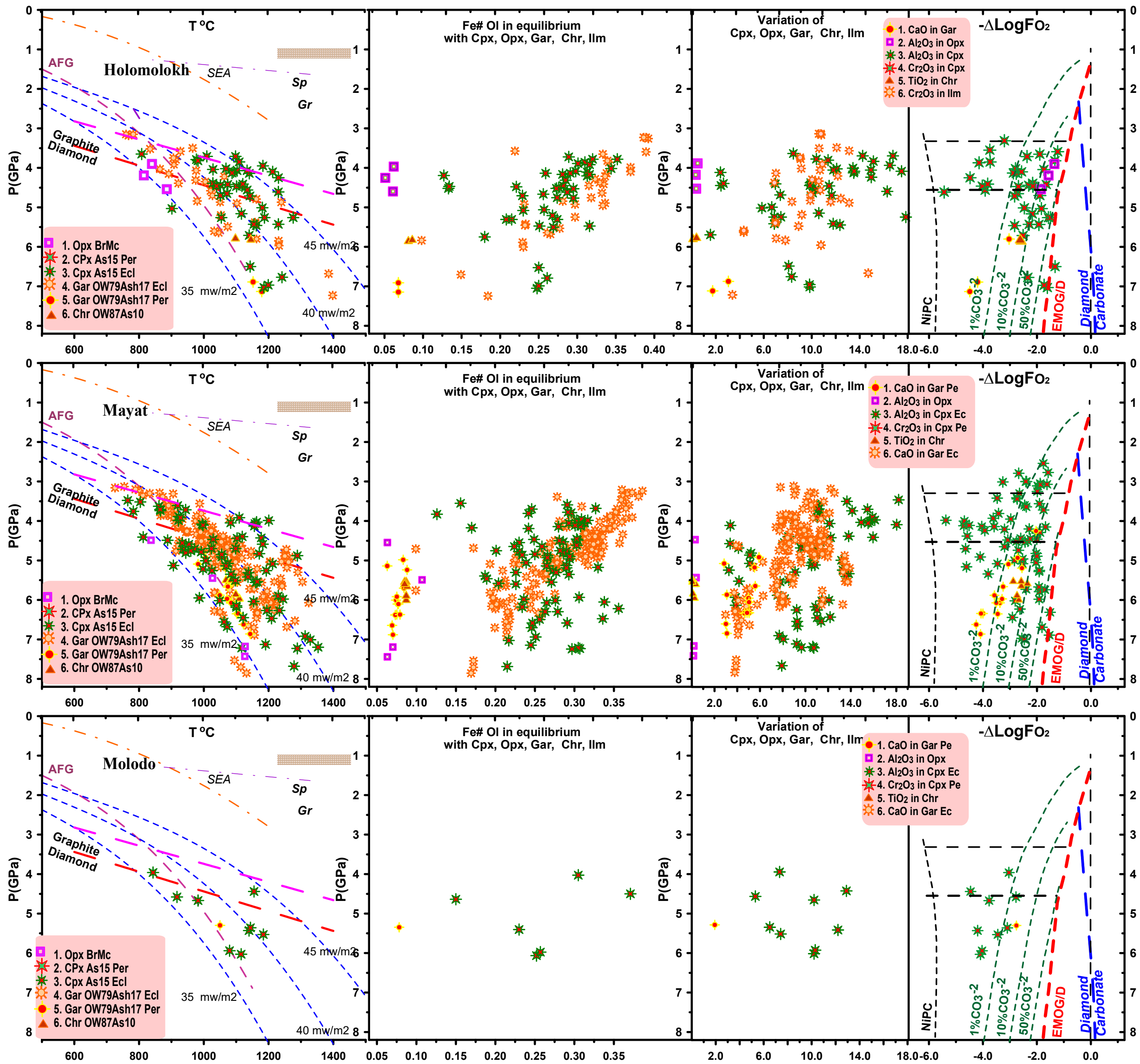

Figure 5. PTXFO2 diagram for diamond inclusions from Ebelyakh kimberlite field Holomolokh (**A**) and Mayat (**B**) and for (**C**) Molodo kimberlite field. Symbols are the same as in Figure 3.

4.1.5. Ebelyakh Field

Inclusions from the North-Eastern Anabar Region from placers of the Mayat river (Figure 5A) and the Holomolokh river [34] (Figure 5B) are similar. The division into two groups shows the individual sources for these two placers. Just as there are few peridotite inclusions in the Nakyn field, harzburgite-type pyropes create a high-Mg trend together with orthopyroxenes and chromites and they mostly come from the Mayat placers (Figure 5B). All together the Cr-rich association gives a linear steep IFDP trend in the Mg-rich part of the diagram. Almandines give the usual trend with increasing gradually together with omphacites, which give a more gradual trend (P-Fe#). Uneven heating in the PT diagram starting from 6 GPa reflects interaction with plume melts. The heated regions are located not only at the base but also in the middle part of the section. In general, the inclusions of these two locations are similar, but may also represent individual sources.

Preprints (www.preprints.org) | NOT PEER-REVIEWED | Posted: 10 August 2021 doi:10.20944/preprints202108.0231.v1

4.1.6. Molodo Field

The diamond placer along the Molodo river also contains mainly inclusions from the diamond of eclogite source (Figure 5C) similar to those from the previous two localities. The plots in P-Fe# and P-Al_2O_3 are very scattered also. They form the dispersed geotherm from 37 to 45 mWm^{-2}. One Cr- pyrope of dunitic type refer to 5 GPA and 37 mWm^{-2} geotherm. All of them suggest very cold conditions. All inclusions are reduced to −3–5 relative QMF buffer.

5. Thermobarometry of Diamond Inclusions of Various Cratons Worldwide.

5.1. Canada

5.1.1. Superior Craton, Wawa Province, Archean Lamprophyres

The diagram for the diamond inclusions only (Figure 6A) reveal rather wide variations of the pyrope garnets which create the broad field at the PT diagram between 40 and 35 mWm- and compositionally varying from sub-Ca (6-7 GPa) to pyroxenitic types at the LAB and in 6 - 4 GPa interval. Eclogitic Cpxs are low in Fe# and are slightly more heated than peridotitic inclusions.

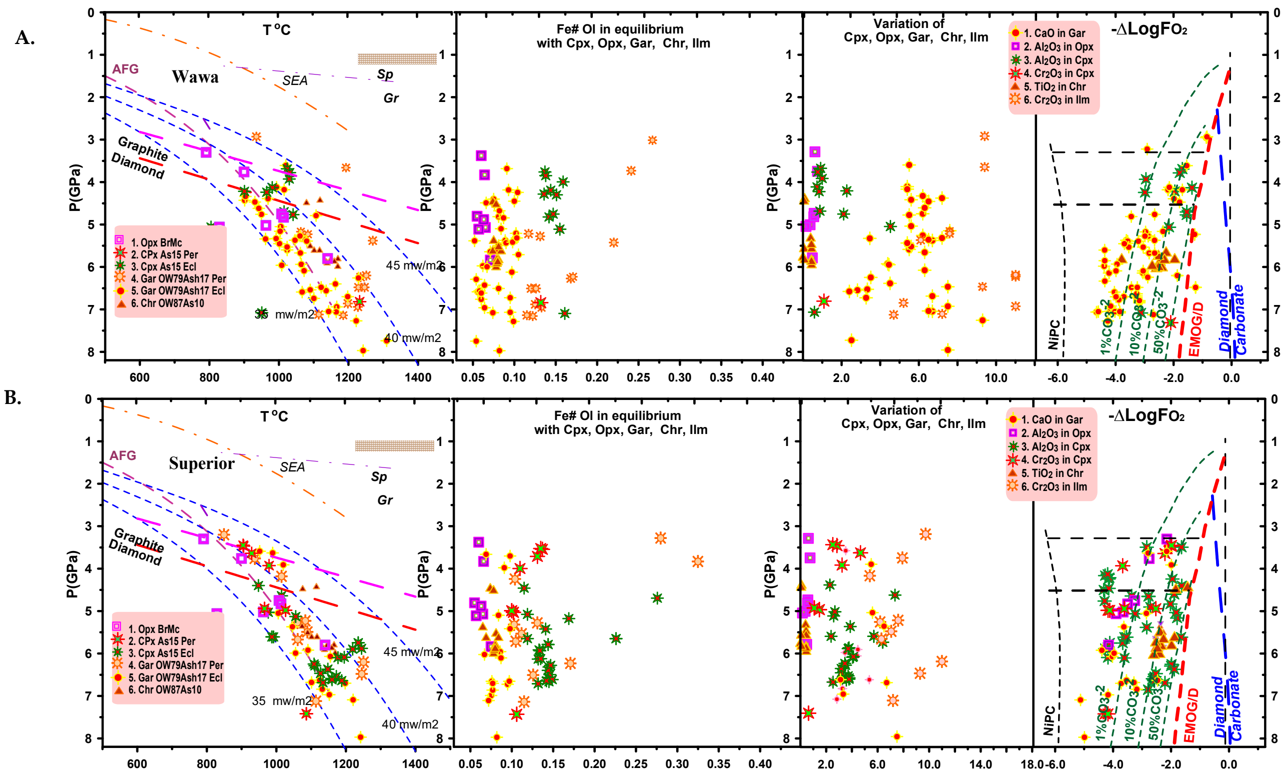

Figure 6. PTXFO2 diagram for diamond inclusions from Wawa lamprophyres (**A**) and Superior craton (**B**. Symbols are the same as in Figure 3.

The Superior craton in Canada contains the most ancient lamprophyre pipes with abundant diamonds and inclusions in the Wawa province. The pipes yield an age of 2.7 Ga [55], which give the possibility to model the structure of the Archean mantle at a time of the worldwide peak of crustal growth accompanied by the subduction and intense percolation of hydrous melts through craton keels. The

The garnet geotherm resembles that from the Archangelsk mantle [180] and is close to the semi-advective type with low-temperature conditions near the LAB and a higher temperature part near the Moho [28]. The pyrope garnets just follow this geotherm and only the Ca-, Fe-rich pyroxenitic group deviates to the high-T conditions. There is some increase in temperature near the LAB. In the P-CaO diagram, there is a split to high-Ca and low-Ca branches. There are at least 4 low-Ca, low-Fe fluctuations in P-CaO -Fe# diagrams for garnets followed by the Opx (Figure 6A).

There are no serious differences between the Archean diamond inclusions and those found in Devonian and Mesozoic and other later kimberlites. Though those from Wawa are, on average, even more, enriched in Fe and Ca than those in younger kimberlites. The clinopyroxenes belong to low-Al and low-Cr groups typical of the depleted cratonic mantle keel. A few follow the ilmenite trend. The Fe-rich pyroxenitic garnets are found in shallow <2 GPa in the upper SCLM. Ilmenites form the long fractionation trend with the continuous increase of Cr_2O_3 to lower pressures [27].

5.1.2. Superior Craton, Phanerozoic Kimberlites

There are significant differences between the Archean diamond inclusions and those found in diamonds from Devonian and Mesozoic and other later kimberlites. Those from Wawa are, on average, even more, enriched in Fe and Ca than those in younger kimberlites.

Diamond inclusions of peridotitic and eclogitic types in the Jurassic (180–174 Ma) Attawapiskat kimberlites [57–59] and Renards kimberlites [55] yield a semi-advective geotherm. The peridotitic inclusions (orthopyroxene and garnet) in the upper part at 3-5 GPa are more fertile types and give the 40–45 mWm^{-2} geotherm than in the LAB where near 7 GPa they are low-temperature (35–37 mWm^{-2}). They coincide in PT conditions with the Mg-rich eclogites falling on the low-temperature branch while the chromites together with the more Fe-rich pyroxenes marking the inflexion to the convective branch (Figure 6B). The Fe-rich eclogitic garnet and clinopyroxenes refer to the middle part of mantle and HT conditions.

5.1.3. Slave Craton

Peridotite inclusions are particularly abundant in diamonds from the Slave craton [66–73] and mainly come from the Lac de Gras cluster (Table 1) [69–73]. Calculations made for inclusion from the Panda pipe Diavik, Jericho and Lac de Gras field together, with a predominance of peridotite diamond inclusions and addition Snap Lake, show rather wide geothermal conditions from the LAB to the graphite-diamond boundary. Many relatively enriched types of pyropes fall on the high-temperature geotherm. In the middle SCLM, they are related to the advective branch. There is an impression that there are several arrays of the convective geotherm which compile together the scattered plot in the middle part. The cold branch is mainly composed of the eclogitic garnets at the deeper part and Cr-pyroxenites in the middle and the uppermost part of the cold branch is marked by the eclogitic Cpx. Cpx from diamond-bearing Mg-type eclogites are located at the 4.5 6 GPa interval and garnets of this type are found to 8 GPa. The IFDP trend compiled together by the Gar and Cpx points is rather steep and starts from 6 GPa, with Fe#Cpx ~0.2 and rises to 3 GPa where Fe#Cpx = 0.3–0.35 (Figure 7A).

5.1.4. Wyoming Craton

Late Devonian kimberlites in Wyoming craton have different type of diamond inclusions In the Sloan pipe [75] the peridotitic inclusions prevail while the Kelsey Lake [74] pipe contains more eclogitic garnets and CPx. Altogether the PT estimates compile the low-T geotherm at 35 mWm^{-2} from 3 to 6 GPa but in the lower part the from 6 to 8 GPa the mantle keel was extremely heated up to 1450 °C and the peridotite Cr- pyropes give the highest temperatures (Figure 7B). They are rather Mg-rich, on average having Fe#Ol 0.07-008. The eclogitic inclusions as common create the IFDP trend with variations of Fe# from 0.15 to 0.37 and pressures from 8 to 3.5 GPa.

Preprints (www.preprints.org) | NOT PEER-REVIEWED | Posted: 10 August 2021 doi:10.20944/preprints202108.0231.v1

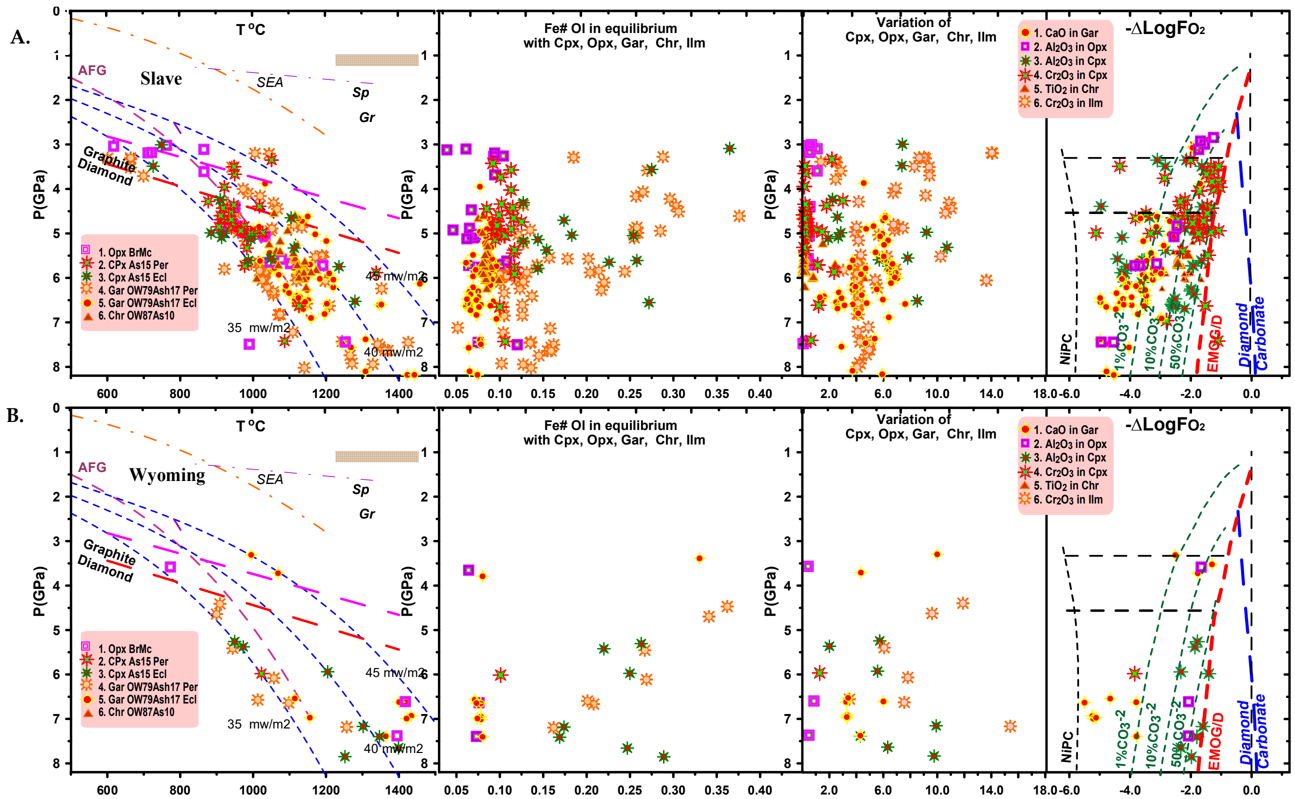

Figure 7. PTXFO2 diagram for diamond inclusions from kimberlites Slave craton (**A**);. (**B**) the same for diamond inclusions from Wyoming craton. Symbols are the same as in Figure 3.

5.2. Africa

5.2.1. Kaapvaal Craton

Data on the inclusions in diamonds the kimberlites from Africa are the most abundant and the Kaapvaal craton with their numerous kimberlite pipes is the most studied (Table 1). The kimberlites are of various ages starting from the Proterozoic like Premier [100,101] to the Mesozoic: Roberts Victor, Letlhakane, Finsch, Jagersfontain, Koffiefontain, Bultfontain, Letseng, Bellsbank, DeBeers Pool, Orapa, Monastery [79–114] and other pipes of similar compositions of the diamond inclusions formed during the Mesozoic episodes of activity, which trace the tails of the major plume events.

Here we represent the separate diagrams for the Proterozoic kimberlites and those from the Mesozoic stage though the varieties of the types from different pipes in the Mesozoic mantle is quite high and we give the separate PTXfO2 diagram (SF1, Fig. 9–24).

We made the combined diagram including the diamond inclusions from the listed Mesozoic pipes to make the diagram for the Mesozoic stage (Figure 8A). The garnet trend there is represented by the dunitic pyropes only, which create the low-T geotherm slightly heated to the lithosphere base. The Opx estimates form several fields there. The HT branch is made by the Fe- enriched (Fe#~0.2) inclusions together with several points of the pyropes garnets at 6–7 GPa related to the plume heating. The several points together with the very low-T eclogitic garnets marking 30–33 mWm^{-2} geotherm. There are three steps of the gently heated geotherms strengthening along the line of the diamond- graphite boundaries. The eclogitic garnets compiles also several branches—One practically repeats the cold geotherm made up by the pyrope garnets the others repeat the OPX stepped geotherms but in a wider range. The PT estimates for omphacites from the eclogites practically repeat the positions of the eclogitic garnets. The chromites similar to Siberian inclusions mainly compiles the heated branch at 6 GPa. The PT points for diamond inclusions of the Cr-pyroxenites follow this estimate.

5.2.1.1. Mesozoic Kimberlites from Kaapvaal Craton

The eclogitic garnets and Cpx formed in the P-Fe# diagrams make up several branches of the IFDP trends on the diagram with the different inclinations joining at the 4.5 and 6 GPa levels possibly they are reflecting the melting and fractionation or interaction of the partial eclogite melts at several levels in the SCLM.

The low-Fe# peridotitic area of this diagram shows several clots referring to the mantle layering. There is the Fe-rich clot for the chromites possibly caused by the protokimberlite melts heating. In the P-fO_2 diagram, there are two major trends. Those very low in fO_2 are related to the ascending high-Mg trend which made the majority of the ancient pyrope sub-Ca garnets. The second event traces the diamond stability field starting from ~−2 ΔQMF.

The special compositions of the DIA in the Voorspoed pipe [96] (Figure SF10) are close to the megacrystic suite (SF1, Figure 1). The trend starts with low-Cr megacrystic garnets, Cpx and Opx. The joint cotectic crystallization pass of Cpx and Gar is tracing to the 45 mWm^{-2} geotherm from 6.5 to 2.8 GP. The Opx-Cpx clot deviates to the lower T conditions possibly refer to the intermediate magmatic source with the joint crystallization of two pyroxenes. The eclogitic garnets and clinopyroxenes are more Fe-rich and yield colder conditions in general.

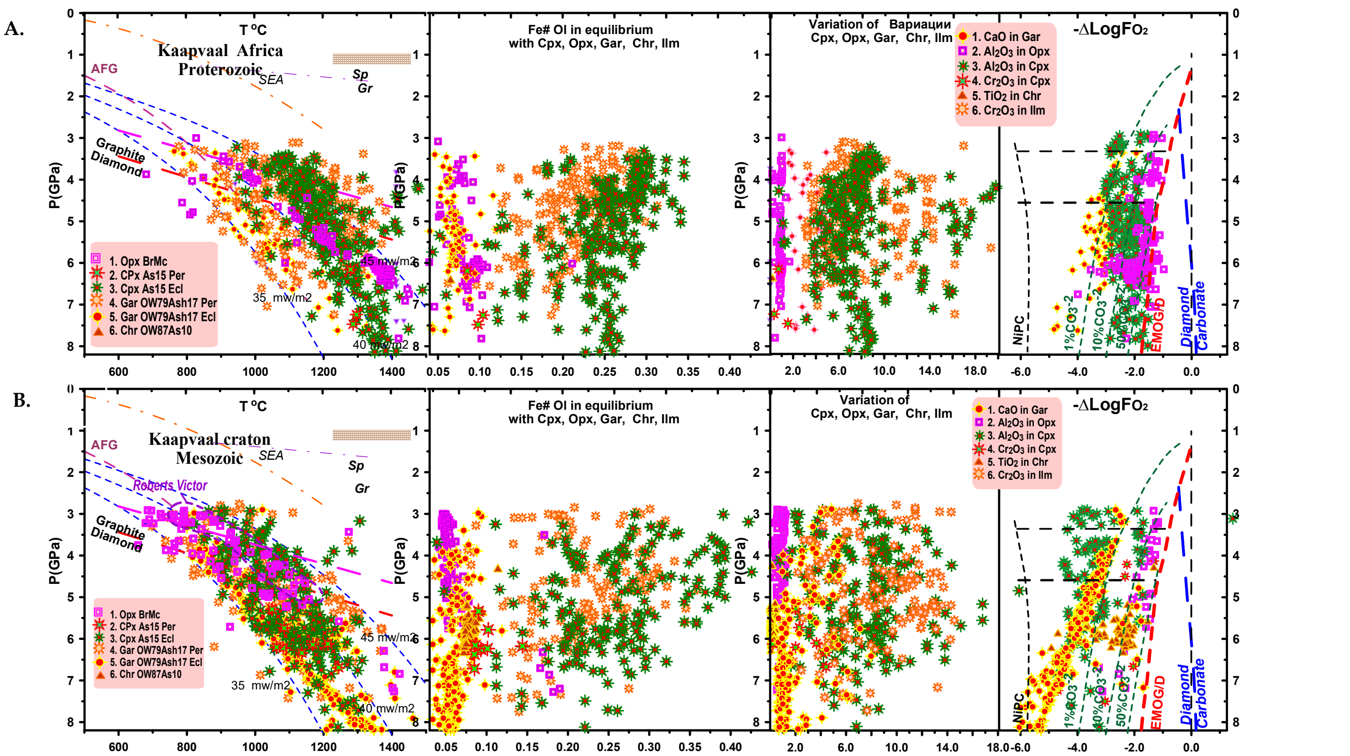

Figure 8. PTXFO2 diagram for diamond inclusions from kimberlites from: (**A**) Kaapvaal craton inclusions in Mesozoic kimberlites; (**B**) Kaapvaal craton inclusions in Proterozoic kimberlites. Symbols are the same as in Figure 3.

5.2.1.2. Proterozoic Kimberlites Kaapvaal Craton

We used the analyses of the diamond inclusions from the most studied pre-Mesozoic pipe—Premier [84–87,101,102] (Table 1). This pipe is famous for extremely large diamonds and the second one for the abundance of the various eclogites dominated also among the diamond inclusions. The PT diagram for this stage represents the hottest material from all studied groups (Figure 8B).

The peridotitic garnets are represented by the relatively fertile harzburgite-lherzolite and even pyroxenitic varieties. The latter refers to ~40 mWm^{-2} close and below 7 GPa and at the common for the Cr-spinels level near 6 GPa and 1200–1350 °C. Garnets of the harzburgitic type gives the colder parts of the PT array showing the layered structure of the mantle keel by the 7–8 low To fluctuations from 3 to 6.5 GPa. The Opx from this stage reveals the HT conditions tracing 45 mWm^{-2} geotherm from 7 to 3 GPa going to 40 mWm^{-2} geotherm at the top/ the relic very low-temperature geotherm ~32 mWm^{-2} which also is traced by the eclogitic garnets and Cpx. The garnets from eclogites are pyrope almandine type and give the low to mean temperature conditions at the lithospheric part of mantle giving the estimates practically coinciding with those for the pyrope garnets. They also create the exclusively HT part of the PT plots to 50 mWm^{-2} from 3 to 6 GPa together with the HT eclogitic Cpx. The latter forms the advective branch from 1450 °C and 8 GPa to 3 GPa to 1250 °C. The other omphacites trace the PT estimates of the pyrope garnets within the lithospheric part of the mantle column.

In the P-Fe# plot, the peridotitic minerals form the nearly coinciding trend with the gradual rise of the Fe# from 0.05 at 3 GPa to 0.11 at 7GPa with the deviations to Mg part for the OPx. The eclogitic CPx are in general more Fe-rich than eclogitic garnets. They are forming the High Fe group (Fe# to 0.4) from 3 to 5 GPa. The deepest Cpx plot to 0.25–8–8.5 GPa. The Al-Ca rich eclogitic minerals are found in all pressure intervals but they create the clot ~5 GPa. The P-fO_2 plot is characterized by the nearly continuous variations of the FO2 in all pressure intervals. The deepest part is characterized by the more oxidized condition near and lower than EMOG buffer. The more reduced conditions give the pyrope garnets with the staring of the array from −5 ΔQMF, which corresponds to the 15 CO3-2 according to [179].

5.2.2. Zimbabwe Craton

There are two main clusters of diamondiferous kimberlites [115] in Zimbabwe craton in River Ranch and Murowa [116,223] pipes. The first contains mostly eclogitic inclusions while in the second peridotitic diamond inclusions prevail.

The ultra-depleted peridotitic DIA [109] give the low-T branch 37 mWm^{-2} from 3 GPa to the LAB and then to 8 GPa is traced mainly by the pyropes of sub-Ca type, higher temperature branch 40 mWm^{-2} is marked by Opx from 5.5 to 3 GPa. The Sp commonly plot at the inflexion from 35 mWm^{-2} at 5 GPa to 40 mWm^{-2} at 6.5 GPa. Eclogitic Cpx are mainly located along the 40 mWm^{-2} geotherm and in the upper part, they go to the 45–50 mWm^{-2} geotherm. The garnets are in general lower temperature and form an LT cluster near 5 GPa and shallower levels are located near the omphacitic PT estimates (Figure 9A).

In general peridotitic minerals have low Fe# 0.05–0.07 but Cr-spinels and some Cpx are more Fe-rich to Fe# = 0.12. Eclogitic minerals are mostly Fe-rich with the Fe# of 0.15–0.2 near the lithosphere base and show a rapid increase up from 6.5 to 3 GPa reaching Fe#~0.36.

Pyropes are extremely depleted in CaO near the LAB and sporadically tend to lherzolite at a shallower level.

5.2.3. Tanzanian Craton.

Diamond inclusions of the Tanzanian craton [190] are mainly of peridotitic type. The PT points of the pyrope garnets are located along the 35–40 mWm^{-2} geotherm from the lithosphere base to 4 GPa. The Opx, Sp and Cpx plot in the upper part (5-3 GPa) and are a bit more high temperature 38–42 mWm^{-2}. The Cpx and Sp are slightly more Fe-rich than depleted garnets (Figure 9B). A few eclogitic diamond inclusions are more high temperature and have Fe# ~0.25–0.30.

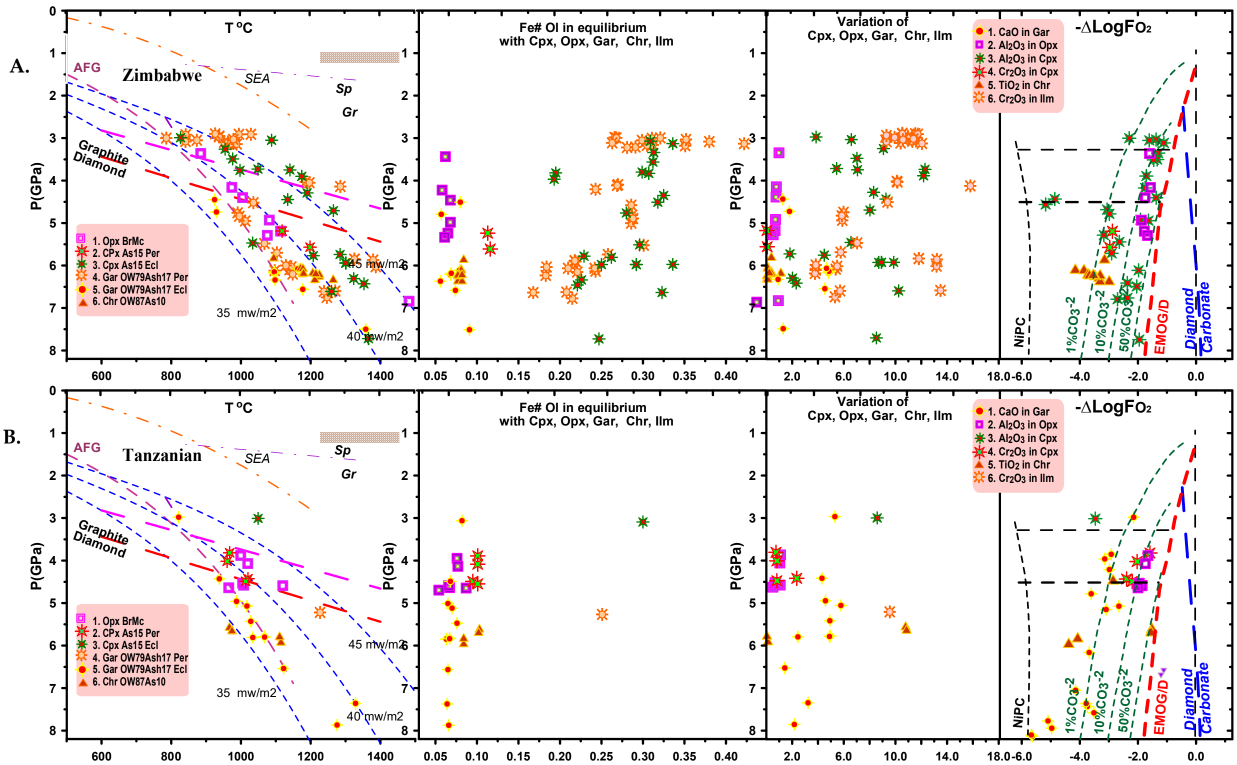

Figure 9. PTXFO2 diagram for diamond inclusions from kimberlites from: (**A**) Zimbabwe craton; (**B**) Tansanian craton. Symbols are the same as in Figure 3.

5.2.4. Magondi Belt

The diagram for the Magondi belt is compiled by the diamond inclusions from the Orapa [15,103-108], Letlhakane [107] and Damtshaa [106] Karowe pipes [190], (Table 1). Pyropes form 4 clusters which represent quite different thermal conditions of 35 and 43–50 mWm^{-2}. Opx scatters between 38–42 mWm^{-2} with a few deviations to HT conditions. Cpxs of low Fe type are forming relatively low-temperature cluster from 4.5 to 6 GPa.

Eclogitic garnets mainly form the broad dense field from 36–43 mWm^{-2} starting from 8 to 3 GPa. Eclogitic Cpxs are even more scattered and have higher temperatures (to 1200 °C) in shallow levels (Figure 10A). But they also formed extremely low-temperature geotherm 33–35 mWm^{-2} from 5 to 7.5 GPa.

The Fe# of the peridotite garnets are different; some pyropes have Fe# 0.15 increasing in the upper level and even higher for Cpx and Opx, The eclogitic garnets show the definite trend of increasing Fe with decreasing pressure. For the Cpx this tendency also exists but they show more scatter.

5.2.5. Limpopo Belt

The diagram for the Limpopo belt is compiled by the diamond inclusions from the Cambrian Venetia pipe [110–112] (Table 1). The diamond inclusions PT estimates also reveal the heated conditions in general and very wide variations of the geothermal conditions. The pyrope garnets give the cold inclined geotherm. Splitting to convective branch at 7 GPa which is common for the other localities. They also reveal the clots for the lherzolitic- pyroxenitic garnets plotting on the 50 mWm^{-2} geotherm at 6.5 GP and at 40 mWm^{-2} with two clusters 6.–5.5 and 7–8 GPa. The Opx conditions and compositions are quite variable. The most Fe-rich Opx are found in the PT plot near the 45 mWm^{-2} geotherm at pressures starting from 6.5 GPa. Some of the trace the graphite- diamond boundary but there are also clots at 35 mWm^{-2} geotherm at 4 GPa. The eclogitic Cpx and garnets reveal the scattering between the 50–35 mWm^{-2}. The relic cold geotherm to 33 mWm^{-2} and even

Preprints (www.preprints.org) | NOT PEER-REVIEWED | Posted: 10 August 2021 doi:10.20944/preprints202108.0231.v1

lower also exist (Figure 10B). The variations for the eclogitic Gar-Cpx at the P-Fe#, in general, are similar to the other fields with the genera ascending IFDP trend and highest Fe# at 3 GPa but there are all Fe variations among the peridotitic and eclogitic compositions(Figure 10B).

The oxidation state of the garnets show very low values for the pyropes (−5.5ΔLogQMF) from the deeper part and much less for the eclogitic garnets (to −2ΔLogQMF).

5.2.6. Congo Craton

For the Congo craton, diamond-bearing eclogites were suggested in Catoca pipe [121]. However, the largest data set for the diamond inclusions was published for the alluvial deposits of the Kasai River, NE Angola [120].

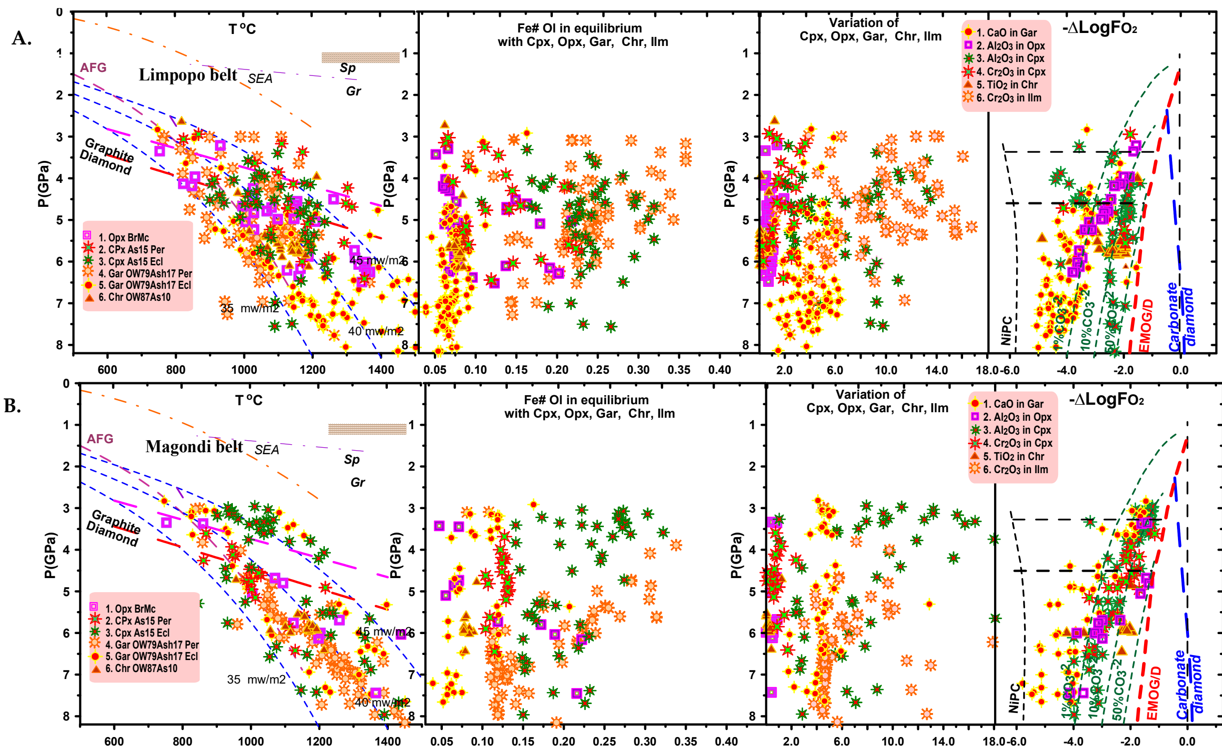

Figure 10. PTXFO2 diagram for diamond inclusions from kimberlites from: (**A**) Magondi mobile belt; (**B**) Limpopo mobile belts. Symbols are the same as in Figure 3.

5.2.7. West Africa Craton.

The PT estimates for the Opx and other minerals, in general, repeat the diagram for the Limpopo belt showing the GPa 1370 °C. The HT branch from conditions is found in the lithosphere base. It was traced also by the pyroxenitic and eclogitic CPx and garnets. Opx show division to 4 discrete pressure intervals. The eclogitic Cpx is divided into several discrete groups. The Fe-rich Cpx reveal the irregularly heated conditions at 4–4.5 GPa. The eclogitic Cpx with garnets the Fe#~0.3 together forms the sub-vertical trend. The Cpx and Ga (Fe#~0.20–0.25) form another cluster in the upper LAB 6–5 GPa (Figure 11A).

In West Africa, some pipes like Koidu [117] while in Akwatia [5] peridotitic diamond inclusions occur more often. The peridotite pyropes are divided by CaO into three groups (Figure 11B). The Opx inclusions and pyropes pyroxenes belong to the advective geotherm which is close to cold 36 mWm^{-2} branch, and at 3 GPa to the heated to 48 mWm^{-2} (Figure 11B) with high scatter near the diamond stability boundaries. Eclogitic Gar and Cpx also repeat this distribution.

The Fe# of Opx varies from 0.06 at the LAB to 0.1 at 3.5 GPa. The eclogitic minerals show two clusters with close values Fe# from ~0.3 and the next ~0.4.

The oxygen conditions vary from −4 to −1.7, being higher near the diamond stability boundary [175,178].

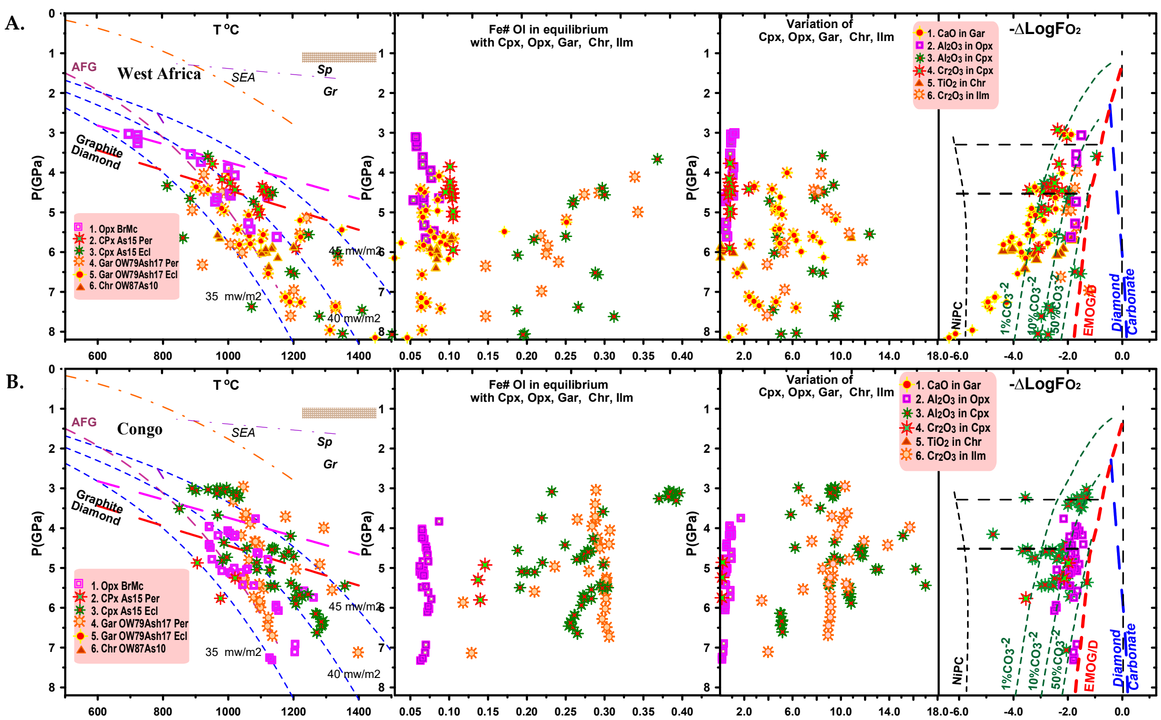

Figure 11. PTXFO2 diagram for diamond inclusions from kimberlites from: (**A**) Congo craton; (**B**) West Africa craton. Symbols are the same as in Figure 3.

5.3. South America

5.3.1. Amazonian Craton

Data for the Amazonian craton of South America are limited [47,48,76–78] (Table 1). The peridotite part is orthopyroxene and garnet, medium- low-temperature (35–40 mWm^{-2}). They have variations of Fe#~0.05–0.10 showing a higher value for Opx from the upper level. Garnets are revealing variations from dunitic to pyroxenitic values. Eclogitic form a fairly high-temperature trend and, as usual, a joint trend of increasing iron content (0.16–0.32) with decreasing pressure from 7.2 to 2.8 GPa. The Cpx are mainly of the high–Al type (Figure 12A).

The amount of published data for Sao Paulo craton are scarce and did not allow construction representative diagram [75].

5.4. Australia

5.4.1. Kimberly craton

Eclogite inclusions of the Kimberley craton, Australia [122–127] (Table 1) vary widely in temperature regime and composition (Figure 12B). The Cr-Mg peridotitic inclusions are moderately Fe-enriched but extremely Al-depleted and give a relatively HT geotherm tracing the advective branch from 7 to 4.5 GPa crossing the 40 mWm^{-2} geotherm. The eclogites are in general lower in temperatures and scatter from 35 to 40 mWm-2 geotherm though the exclusively HT varieties also occur. They also scatter in the P-Fe# plot (Figure 12B).

 doi:10.20944/preprints202108.0231.v1

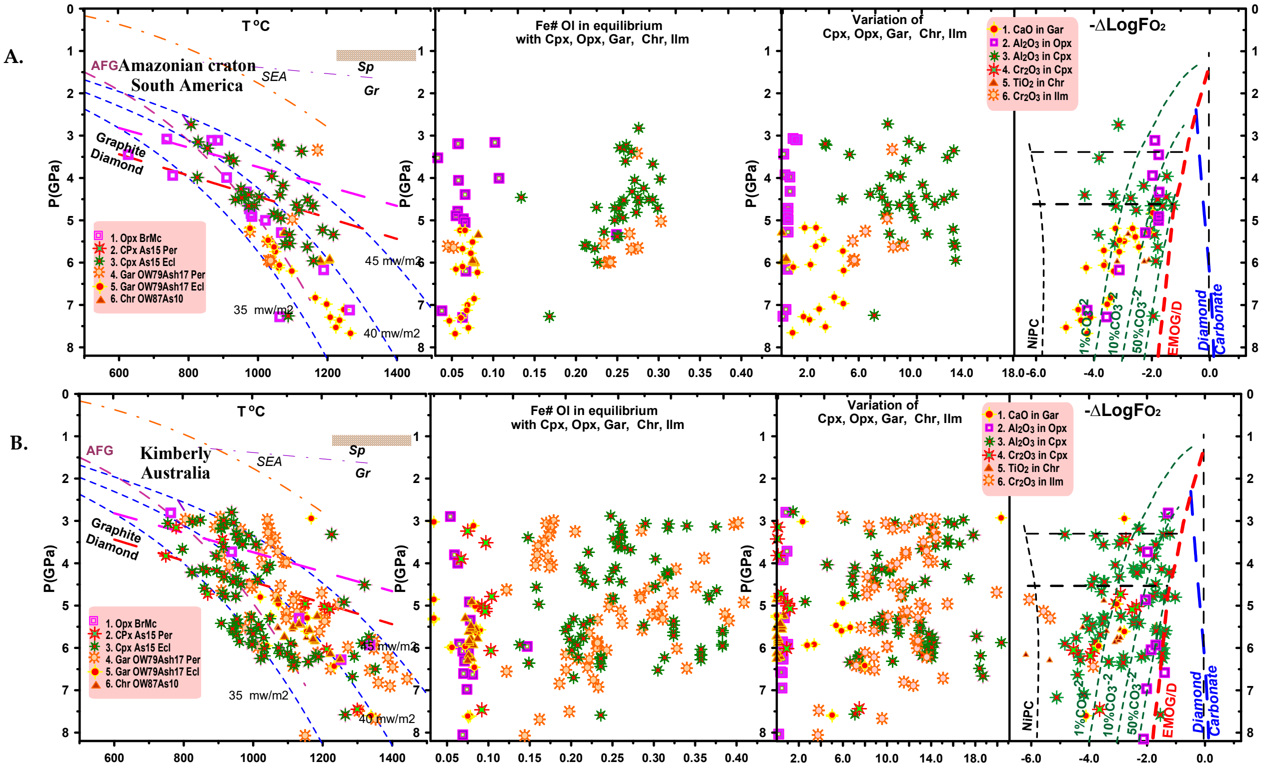

Figure 12. PTXFO2 diagram for diamond inclusions from kimberlites from: (**A**) Amazonian craton, South America; (**B**) Kimberly craton, Australia. Symbols are the same as in Figure 3.

5.5. Eastern European Craton

For the Eastern European craton kimberlites are found in the Baltic Shield [151] and the Arkhangelsk province [148–150]. Eclogitic garnet inclusions are located along the 36 mWm^{-2} geotherm while the omphacites plot between 40 and 45 mWm^{-2} peridotitic chromites are located near 6 GPa at 3.8 mWm^{-2}. The eclogitic Gar and Cpx DIA together form the IFDP trend. It is less steep for garnets and more scattered and more HT for the Cpx (Figure 13A).

The eclogitic Gar and Cpx DIA together are forming the IFDP trend. It is less steep for garnets and more scattered and more HT for the Cpx (Figure 13A).

5.6. Ural Mobile Belt

In Polar Urals [150–152], a few peridotite DIA were found. Eclogite omphacites show higher temperatures than garnets. The compositions of the prevailing eclogitic and Cpx give together the relatively HT conditions but garnets are determined the lower T scattered geotherm below 40 mWm^{-2}. The Cpx give the advective geotherm from the lithosphere base to 3 GPa.

The Cr-Mg trend is relatively scarce and represented by the lherzolite-harzburgite garnets chromites (5–6 GPa) and Opx at 4 GPa (Figure 13B).

Preprints (www.preprints.org) | NOT PEER-REVIEWED | Posted: 10 August 2021 doi:10.20944/preprints202108.0231.v1

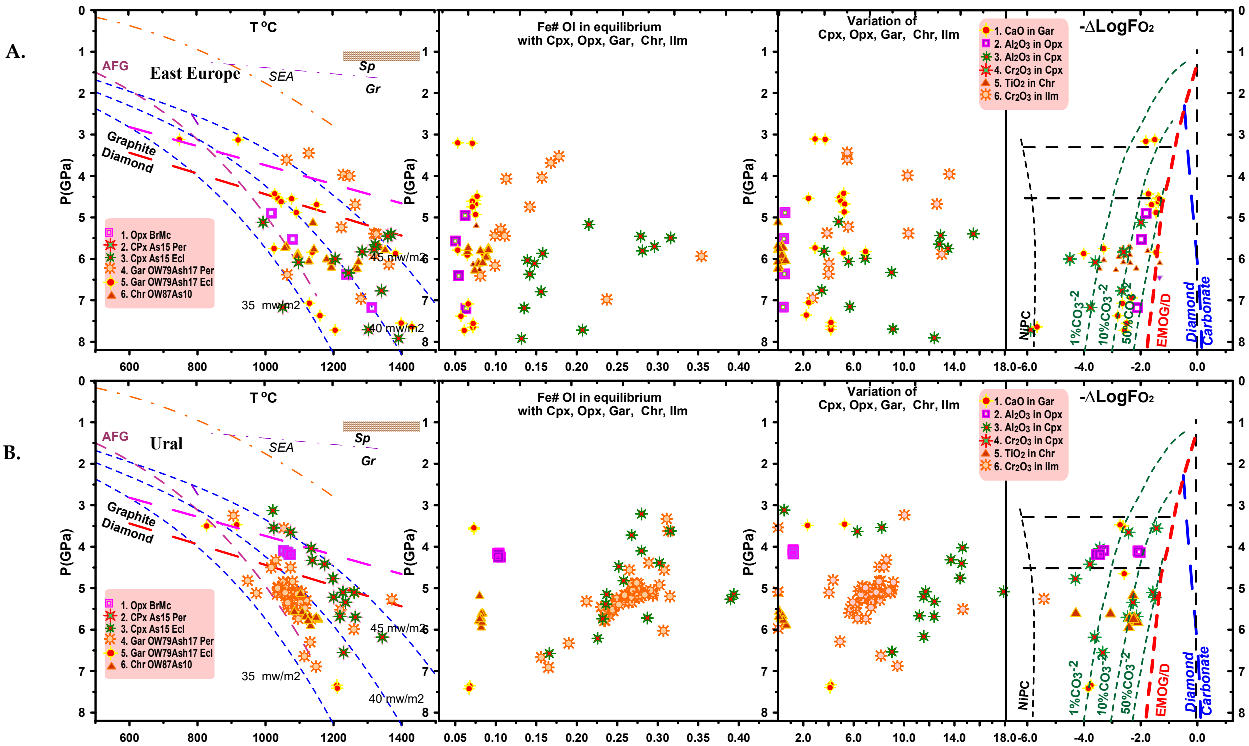

Figure 13. PTXFO2 diagram for diamond inclusions from kimberlites from: (**A**) East European craton; (**B**) Ural mobile belt. Symbols are the same as in Figure 3.

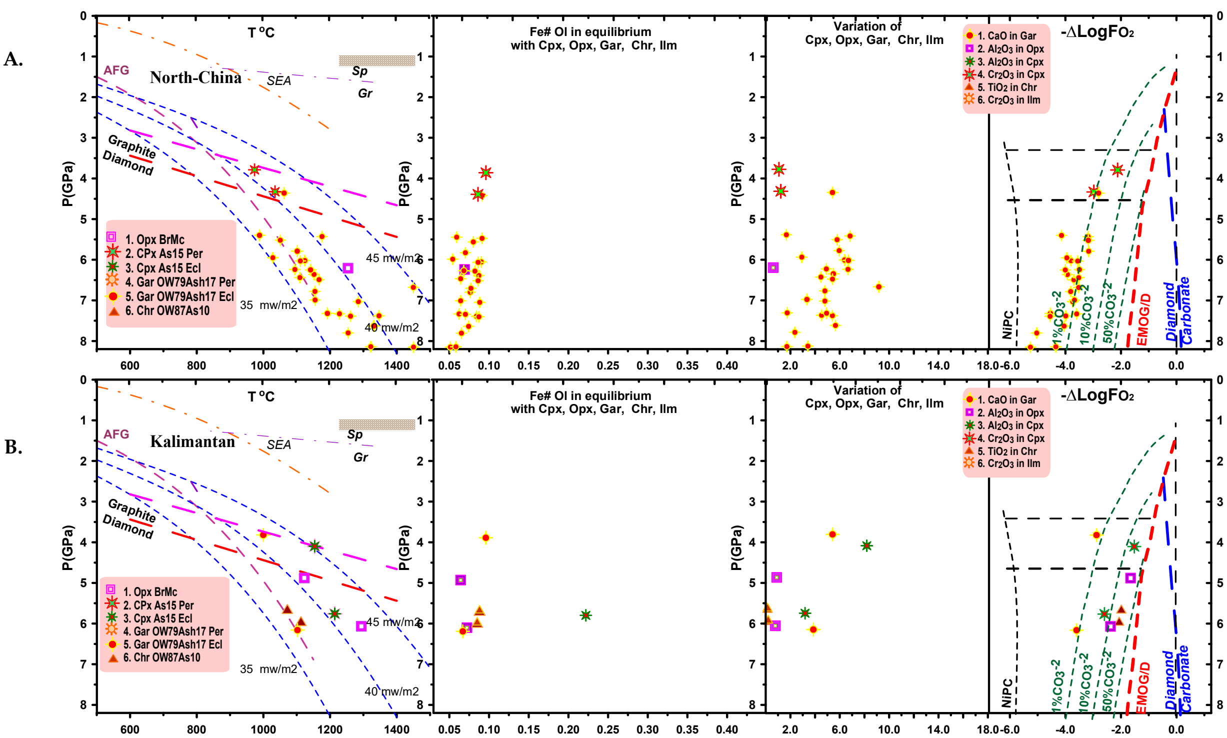

Figure 14. PTXFO2 diagram for diamond inclusions from kimberlites from (**A**) North-China craton. (**B**) Kalimantan Island. Symbols are the same as in Figure 3.

5.7. Sino–Korean (North China) Craton

In North China craton the only known DIA are from Shengli, N 50 pipes are mainly Cr- pyrope garnets [153]. They vary from dunitic and harzburgitic to lherzolitic varieties. In the PT plot, they give ~37 mWm^{-2} geotherm with the more heated to 40 mWm^{-2} below 7 GPa, though this geotherm is sporadically traced to 4 GPa (Figure 14A). Only one sample is heated to 45 mWm^{-2}. The clinopyroxenes plot in the deepest part of the mantle column and Opx at 6 GPa. The Fe# of the olivine in equilibrium with the garnets is varying from 0.05 to 0. 1, the latter values are typical of the Cpx also while the Opx show Fe#~0.08. The CaO content of the garnets is rising with the decreasing pressure. Thus the DIA from the Sino-Korea craton represents a very deep heated and relatively fertile or fertilized mantle source of diamond.

5.8. Kalimantan

In Borneo kimberlites or lamproites were not found alluvial diamond inclusions [154] give rather high-temperature conditions for both peridotitic and eclogitic suits. Only pyrope garnet and chromites drop the 38 mWm^{-2} geotherm at 6 GPa. The Opx, eclogite and pyroxenite PT estimates are plotting between 40 and 45 mWm^{-2} geotherm (Figure 14B).

6. Discussion

6.1. Distributions of Different Types of Mantle Inclusions in Mantle Sections

It is clear from the diagrams for all data set (SF1, Fig.1-3) that the amount of the Opx, as well as the amount of Cr-bearing, pyroxenites commonly, increase towards the middle part of mantle columns. It seems that the degree of melting and the concentration of the melts greatly increases in the so-called pyroxenitic layer [188] in the middle SCLM. Comparing the diagrams for the eclogitic clinopyroxenes and garnets it is also clear that garnets more frequently occur in the lower parts of SCLM and clinopyroxenes are tending to the middle part. This possibly reflects the effect of the migration upward of the light part of the ancient adakitic melt formed after the remelting of the primary eclogites and the effect of garnet fractionating at the lower part of SCLM.

In some mobile belts like Urals, Khapchan, in SCLM beneath Premier pipe the Cpx form more HT branches despite commonly eclogite garnets and omphacites form a joint trend. This discrepancy may be explained by the different reactions of the Gar and Cpx to the heating, garnet is less affected by the influence of magmas and in xenoliths, they are often un-equilibrated [184]. Even in the same locality, they may refer to the different times of formation.

Chromites are mostly concentrated just above the LAB (SF1, Fig.1-7) which is the mechanical layer caused by magmatic fracturing produced by protokimberlite and kimberlite magmas and it seems that most spinels are formed during the latest magmatic event in the SCLM and often trace the inflexion of the convective geotherm. Such conditions 1140-1200 - 6 GPa were determined for chromites by the elastic barometry [192].

Fe-type eclogites are distributed frequently in the mantle column just the middle part of the mantle column. The structure and composition of the upper and middle parts of SCLM essentially differ and are highly likely that the upper SCLM part with the Fe-eclogites at the basement was created in Early Archean time. The IFDP trends may also be the results of the evolution of ascending eclogitic partial melts produced during subduction and the later influence of superplumes and plumes. This evolving melt may become more Fe-rich in the upper levels.

However, such trends may be also produced by sequential melting of subducted oceanic gabbroic cumulates. The Ca-Al eclogites tend to concentrate within the 5–6 GPa interval but may occur at any level.

Preprints (www.preprints.org) | NOT PEER-REVIEWED | Posted: 10 August 2021 doi:10.20944/preprints202108.0231.v1

6.2. Geothermal Regimes of Diamond Formation

It is generally accepted that the mantle has the same geotherms for the same locality with the inflexion and at the lithosphere base. Commonly xenoliths geotherm is rather cool and refers to 38 mWm^2 [4]. But even beneath Udachnaya, the xenoliths give quite different thermal conditions for each group of peridotites and eclogites the single geotherm is produced by the rather old set of thermobarometers. The correct estimates give rather cold conditions for dunites (35 mWm^2). And pyroxenites related to plume melts give hot geotherm to 45 mWm^2 [28].

The correct determination using Opx and Cpx methods give a rather wide range of conditions and geothermal gradients from 35 to 45 mWm^2 [8,9,38, 159,160]. Relatively cold 40 mW/m^2 were determined for the peridotitic DIA from Premier pipe [38]. The super adiabatic plum related geotherm created by Bushveld plume influences and refer mainly to pyroxenitic and eclogitic inclusion. Our estimates show HT regime for Premier pipe DIA (SF1, Fig.11). The olivine thermobarometry [193] for DIA from Akwatia produces 40 mWm^2 geotherm. The thermobarometry of fluid-related minerals [194] suggest rather cold conditions of diamond formation.

Diamonds belonging to the different associations formed at the time distance from 3.5 GA [16,195] to kimberlite eruptions and thus they give the different PT regime of formation. The CPx diamond inclusions in the Urals are dated as Devonian [154] as well as in Eastern Europe craton c time close to host kimberlite eruption and they trace rather hot geotherm branches which differ from the garnet geotherms.

The coldest geotherm near 35 mWm-2 and lower is determined everywhere for sub-Ca pyrope garnets [196] which were created 3-2.7 GA [18,19].

6.3. PT Conditions and Presence of Metastable Associations in Diamonds

One of the newest conclusions of this research is that diamond PT conditions of most diamonds are estimated within the diamond stability field [166] many types are at the upper boundary of upper the diamond stability field [167] and even re-estimated version [164]. And this is not a mistake of the new methods [21–27] because all existing barometers including Al-in-Opx [164], Cr-in-Cpx C [158] barometer as well as [11,182] and [21–24] methods give for >10% of inclusions the pressure estimates upper than determined graphite-diamond boundary [163,164]. It is necessary to say that some inclusions like K-feldspar [97] also suggest rather low-pressure conditions. There is a suggestion about the crust conditions for gemstone diamonds [197]. We do not support this idea but should emphasise that most of the natural associations reveal the presence of volatiles, fluids [198–202] and growth in metasomatic associations [5,6,201]. This is supported by the experiments [203–204].

6.4. Influence of Protokimberlitic Magmas

Boyd F.R. and colleagues [4] showed the inflexions of the geotherms at the LAB and the heating of sheared peridotites. The advective geotherms mark the interaction with the ascending protokimberlitic melts. The HT geotherms like for Premier pipe [38] means that most of the diamonds in this region were growing during the plume event. All chromite inclusion at the geotherm inflexion at the LAB should reflect the influence of protokimberlites.

Commonly the protokimberlite magmas create Ti-rich associations which are rare among the DIA but dominate among the Voorspoed DIA [96] which are mainly composed of the megacrystic association [187]. Very often large well-shaped diamonds of type II [191] are determined as megacrysts. There is also geochemical evidence for the crystallization of diamonds from protokimberlites [205-207] supported by ages [208].

There are many shreds of evidence that the diamonds were created at the vicinity of the magmatic systems and chambers and mechanically capture minerals from the magmatic-fluid mush of different associations. The magmatic systems cold increase the pressure around the magmatic system due to the hydraulic effect transferring it from the depth

Preprints (www.preprints.org) | NOT PEER-REVIEWED | Posted: 10 August 2021 doi:10.20944/preprints202108.0231.v1

(Figure 15). Hydrous conditions and extra fluid pressure could expand the diamond stability field to lower pressure. Commonly the most active interaction with the protokimberlite melts occurs near the LAB which is the physical boundary of the minima of the ultimate strength of olivine at the presence of hydrous melts [209]. And the division on the lithospheric and asthenospheric diamonds is only in presence of the protokimberlitic melts at diamond forming media. The diamond inclusions sometimes do not refer to the diamond-forming media but represent the mechanically trapped inclusions of crystal mush having lithostatic characteristics. And this explains the presence of mixed paragenesis [210].

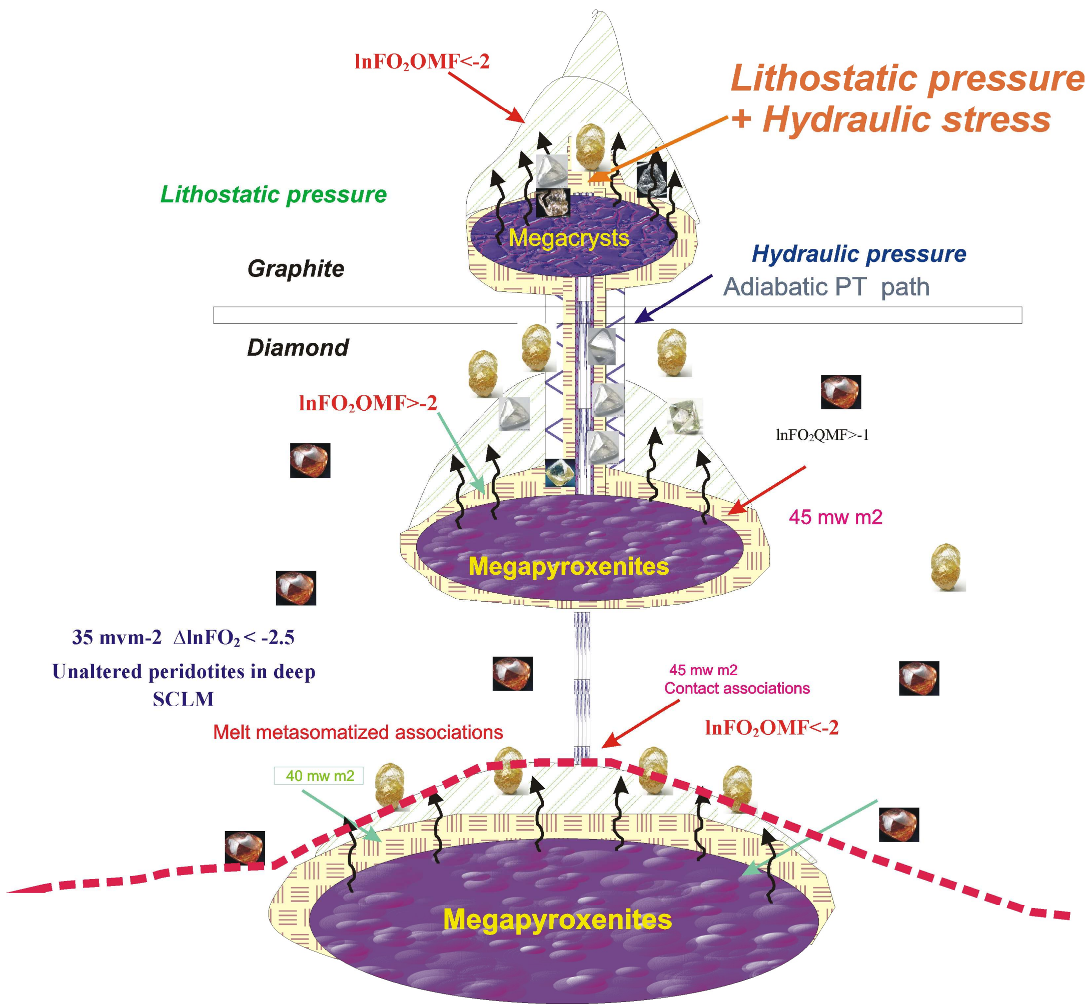

Figure 15. Scheme of diamond growth below and above the diamond–graphite boundary.

6.5. Evolution of Diamond Forming Processes in Time.

The first questions about mantle reconstructions with the DIA and are: have they evolved over time? How do they reflect the conditions of the cratonic growth and evolutions [2008, 2010-214].

The ages of diamond formation vary from Archean to the time of intrusion of the host kimberlites [57,106,107,112,119,195,208,211,220]. Comparison between the Wawa DIA [216] and those from younger kimberlites suggests that such an evolution can be observed. The pyrope garnets from Wawa lamprophyres are more Fe-rich in general, excluding some ultra-depleted compositions. The Ca-rich varieties are more abundant than

Preprints (www.preprints.org) | NOT PEER-REVIEWED | Posted: 10 August 2021 doi:10.20944/preprints202108.0231.v1

among the later Proterozoic and Phanerozoic kimberlites. They do not form the continuous trends and geotherms as is common for other cratons such as Siberia or South Africa but trace four separate levels. Though the crystallization of megacrystalline dunites beneath Udachnaya [212] also refer to separate levels [21-27,216]. Our opinion that the low-Ca garnet [221] LT geotherms were formed due to the hydrous subduction-related melt percolation in dunitic channels [214-221] possibly occurred during the major event of growth of the continental crust 3.0–2.7 Ga [18,19,210,222], accompanied by hydrous melt percolation and generation of dunite channels in the mantle. Chromites in Wawa lamprophyres are similar to those from younger kimberlites but are slightly more Fe-rich.

The Proterozoic kimberlites from the Kaapvaal are much higher temperature but this is probably due to the influence of the Bushveld superplume which also caused extensive removal of all the ultra-depleted dunitic garnets [38,208]. The eclogitic inclusions in Premier (SF1, Fig.11) are very HT and also seem to be mainly re-melted. Though some of them keep subduction characteristics [223]. This is less pronounced for the Mesozoic pipes though the Roberts-Victor inclusions (SF1, Fig.16) are also HT by eclogite xenoliths show less influence of the plume melts and as reported [94] and keep their primary subduction features but also they are relatively high temperatures compared to DIA from the other Mesozoic pipes in South Africa. In general, the Proterozoic kimberlites contain more eclogitic inclusions of various types. The study of the eclogitic diamonds gives information about both plume [223,224] and subduction [225-228] processes and the formation of the ancient crust [209–215].

It is possible that the high dispersion of the geothermal trend forming several arrays of the convective branch was formed by the thermal perturbation under plume events [214,219,224,228] from 2.5. to 2.0 Ga beneath the Slave [13] and Kaapvaal craton [38] and later to the rifting at 0.7 Ga, possibly to the protokimberlite event which gives the separate trajectories of the melt movements [230]. The viscosity of the carbonatitic melts related to the plumes is very low [231] which allow the pervasive melt percolation and creation of advective geothems.

6.6. Dependence of DIA Compositions on the Position Within the Cratons and terrain type

In the SCLM beneath South Africa, pyrope garnets from the off-craton Limpopo and Magondi belt show more variable compositions than in the Kaapvaal craton. They also contain more eclogitic and pyroxenitic types of inclusions. This is be a common feature o the suture zones between terrains [232]. If we compare the cores of cratons with the marginal parts, the amount of ultra-depleted pyropes is higher in the centres, and they contain more Opx relative to Cpx. Suture zones, such as the Khapchan zone in Siberia, contain mainly eclogitic inclusions of Cpx and Gar [34]. This is possible because suture zones contain the inclined remnants of subducted slabs and are the location of the transfer of eclogitic partial melts. The thermal regime of the mobile belts commonly has very high variations from the cold to very high-temperature conditions (~35–50 mWm^{-2}).

The PT conditions estimated for the different terranes in Yakutia (Siberia) are quite variable [21-28]. The late Archean Early Proterozoic granulite-orthogneiss Daldyn and Alakit terranes m1arking ancient suture zones differ mainly in the amount of pyroxenitic pyropes which are abundant in the East Daldyn (Alakit) terrane [33]. They all demonstrate the folded mantle structure [25]. The sub-terrains such as Alakit and Daldyn (and other examples) demonstrate the difference in the eclogites (prevailing B- oceanic type Daldyn) and dominating types of Cr-diopsides more depleted for the latter possibly referring to the continental arc and abyssal oceanic material, respectively. In the granite-greenstone terranes such as Magan, Berikte terranes the prevailing type is peridotitic [128-131]. They contain OPx and Cr-Cpx in equal amounts. The eclogites tend to have more acid and pelitic compositions. The granulite-orthogneiss terranes like Daldyn terrane contain highly variable eclogites pyroxenite and peridotite compositions in nearly equal amounts [133-140].

The suture and accretion terranes concentrate mainly on mafic eclogites and basic pyroxenites. In the Khapchan terrane, most diamond inclusions are of the eclogitic type

 doi:10.20944/preprints202108.0231.v1

like in the Ebelyakh field [34]. The mobile belts like the Urals [154], Magondi [15,105-108] and Limpopo [110–112] belts which are suture zone having cratonic keels in the basement demonstrate similar features.

The perspectives of the study of diamond inclusions are widely discussed. It is evident that the oxidation state is the major factor of diamond formation [233]. They may characterise the source and possible host melts [234] and processes of their formation and as well as geodynamic regimes in ancient times [235-240].

7. Conclusions

1. The PT conditions of diamond inclusion and associations from the Proterozoic, Paleozoic and Mesozoic kimberlites differ.
2. There are regularities in in-depth distributions of DIA in mantle columns. Pyroxenitic inclusions are tending to concentrate in the middle part of the mantle section as well as Fe-rich eclogites. Chromites and often Ca-Al rich pyropes trace the lithosphere-asthenosphere boundary.
3. Commonly the peridotitic inclusions are lower temperature than pyroxenitic and eclogitic varieties, subjected to the plume influences.
4. The extra pressures by the hydraulic effect of protokimberlites could expand the intervals of the diamond creation.
5. Diamond inclusions in off-craton settings and mobile belts show higher temperature conditions and prevailing pyroxenitic and eclogitic assemblages.
6. There is an essential difference in compositions of diamond inclusions depending on their geodynamic specialization.

Supplementary Materials: The following are available online at www.mdpi.com/xxx/s1,

Authors Contributions: Sample acquisition, A.M.L. and Z.V.S.; conceptualization, I.V.A. and A.M.L.; validation, I.V.A., A.M.L. and Z.V.S. formal analysis, I.V.A., A.M.L. and Z.V.S.; investigation, I.V.A., A.M.L. and Z.V.S.; resources, I.V.A.; data curation, I.V.A., A.M.L. and Z.V.S.; writing—original draft preparation, I.V.A.; writing editing I.V.A. and H.D.; supervision, I.V.A.; project administration, I.V.A.; funding acquisition, I.V.A. All authors have read and agreed to the published version of the manuscript.

Funding: Ministry of Science and Higher Education of the Russian Federation. Supported by RFBR grants 19-05-00788; 16-05-00860a. Work is done on the state assignment of IGM SB RAS.

Data Availability Statement:

Acknowledgements: Authors are grateful for the materials from the dissertations of L.Reimers, L. Pokhilenko and to M.Kopylova, N.Korolev and materials of research; to of S.Aulbach for the consultations and materials and to D. Philips and anonymous reviewers commented on this article.

Conflicts of Interest: The authors declare no conflict of interest.

 doi:10.20944/preprints202108.0231.v1

References

1. Pearson, D.G.; Shirey, S.B.; Harris, J.W.; Carlson, R.W. A Re–Os isotope study of sulfide diamond inclusions from the Koffiefontein kimberlite S.Africa: constraints on diamond crystallisation ages and mantle Re–Os systematics. *Earth Planet. Sci. Lett.* **1998**, *160*, 311–326.
2. Boyd, F.R.; Pearson, D.G.; Nixon P.H.; Mertzman S.A. Low-calcium garnet harzburgites from southern Africa: their relations to craton structure and diamond crystallization. *Contrib. Mineral. Petrol.* **1997**, *113*, 352-366.
3. Boyd, F.R.; Finnerty, A.A. Conditions of origin of natural diamonds of peridotite affinity. *J. Geophys. Res.* **1980**, *85*, 6911–6918.
4. Boyd, F.R.; Pokhilenko, N.P.; Pearson, D.G.; Mertzman, S.A.; Sobolev, N.V.; Finger, L.W. Composition of the Siberian cratonic mantle: evidence from Udachnaya peridotite xenoliths. *Contributions to Mineralogy and Petrology* **1997**, *128*, 228–246.
5. Stachel, T.; Harris, J. W. Diamond precipitation and mantle metasomatism – evidence from the trace element chemistry of silicate inclusions in diamonds from Akwatia, Ghana. *Contributions to Mineralogy and Petrology* **1997**, *129*, 143–154.
6. Sobolev, N.V. Deep-Seated Inclusions in Kimberlites and the Problem of the Composition of the Mantle. *Amer. Geophys. Union, Washington, DC* **1974,** 279 p.
7. Stachel, T.; Luth, R.W. Diamond formation — Where, when and how? *Lithos* **2015**, *220–223*, 200–220.
8. Stachel, T., Harris, J.W. The origin of cratonic diamonds — Constraints from mineral inclusions. *Ore Geology Reviews*, **2008**, *34*, 5–32
9. Griffn, W. L.; Gurney, J. J.; Ryan, C. G. Variations in trapping temperatures and trace elements in peridotite-suite inclusions from African diamonds: evidence for two inclusion suites, and implications for lithosphere stratigraphy. *Contributions to Mineralogy and Petrology* **1992**, *110*, 321–336.
10. Griffin, W.L; Ryan C.G. 1996. An experimental calibration of the ``nickel in garnet'' geothermometer with applications, by D. Canil: discussion. *Contrib Mineral Petrol.* **1996**, *124*, 216–218.
11. Ryan, C. G.; Griffin, W. L.; Pearson N. J. Garnet geotherms: Pressure-temperature data from Cr-pyrope garnet xenocrysts in volcanic rocks. *J. Geophys. Res. B.* **1996,** *101/3*, 5611-5625.
12. Aulbach, S.; Stachel, T.; Creaser R.A.; Heaman, L.M.; Shirey, S.B.; Muehlenbachs K.; Eichenberg, D.; Harris, J.W. Sulphide survival and diamond genesis during formation and evolution of Archaean subcontinental lithosphere: A comparison between the Slave and Kaapvaal cratons. *Lithos* **2009**, *112, S2*, 747-757.
13. Aulbach, S.; Heaman, L.M.; Stachel, T., 2018, The diamondiferous mantle root beneath the central Slave craton: *Society of Economic Geologists, Special Publication* **2018**, *20*, 319–341.
14. Aulbach, S.; Stachel, T.; Viljoen, K.S.; Brey, G.P.; Harris, J.W. Eclogitic and websteritic diamond sources beneath the Limpopo Belt – is slab-melting the link. *Contributions to Mineralogy and Petrology* **2002**, *143*, 56–70.
15. Cartigny, P.; Harris, J.W.; Javoy, M. Eclogitic, peridotitic and metamorphic diamonds and the problems of carbon recycling – the case of Orapa (Botswana). *In: J.J. Gurney, J.L., Gurney, M.D. Pascoe and S. H. Richardson (Editors), Proceedings of the VIIth International Kimberlite Conference, Red Roof Design, South Africa* **1999**, *1*, 117–124.
16. Pearson, D.G.; Shirey, S.B. Isotopic dating of diamonds. In Application of Radiogenic isotopes to Ore Deposit *Research and Exploration (eds. D.D.Lambert and RuizJ.). Society of Economic Geologists, Boulder* **1999**. *12*, 143–172.
17. Jagoutz, E.; Lowry, D.; Mattey, D.; Kudrjavtseva, G. Diamondiferous eclogites from Siberia: Remnants of Archean oceanic crust. *Geochim. Cosmochim. Acta* **1994**, *58*, 5195–5207.
18. Pearson, D.G. The age of continental roots. *Lithos* **1999**, *48*, 171–194.
19. Pearson, D. G.; Snyder, G.A.; Shirey, S.B.; Taylor, L.A.; Carlson, R.W.; Sobolev, N.V. Archaean Re–Os age for Siberian eclogites and constraints on Archaean tectonics. *Nature* **2005**, *374*, 711–713
20. Nimis P. The pressures and temperatures of formation of diamond based on thermobaromerry of cromian diopside inclusions. *The Canadian Mineralogist* **2002**., *40*, 871-884.
21. Ashchepkov, I.V.; Pokhilenko, N.P.; Vladykin, N.V.; Logvinova, A.M.; Kostrovitsky, S.I.; Afanasiev, V.P.; Pokhilenko, L.N.; Kuligin, S.S.; Malygina, L.V.; Alymova, N.V.; Khmelnikova, O.S.; Palessky, S.V.; Nikolaeva, I.V.; Karpenko, M.A.; Stagnitsky, Y.B. Structure and evolution of the lithospheric mantle beneath Siberian craton, thermobarometric study. *Tectonophysics* **2010**, *485*, 17–41.
22. Ashchepkov, I.V.; André, L.; Downes, H.; Belyatsky, B.A. Pyroxenites and megacrysts from Vitim picrite-basalts (Russia): Polybaric fractionation of rising melts in the mantle? *Journal of Asian Earth Sciences* **2011**, *42*, 14–37.
23. Ashchepkov, I.V.; Rotman, A.Y.; Somov, S.V.; Afanasiev, V.P.; Downes, H.; Logvinova, A.M.; Nossyko, S.; Shimupi, J.; Palessky, S.V.; Khmelnikova, O.S.; Vladykin, N.V. Composition and thermal structure of the lithospheric mantle beneath kimberlite pipes from the Catoca cluster, Angola. *Tectonophysics* **2012**, *530–531*, 128-15
24. Ashchepkov, I.V.; Ntaflos, T.; Logvinova, A.M.; Spetsius, Z.V.; Downes, H.; Vladykin, N.V. Monomineral universal clinopyroxene and garnet barometers for peridotitic, eclogitic and basaltic systems. *Geoscience Frontiers* **2017**, *8*, 775–795
25. Ashchepkov, I.V. Program of the mantle thermometers and barometers: usage for reconstructions and calibration of PT methods. *Vestnik Otdelenia nauk o Zemle RAN* **2011,** *3*, NZ6008.
26. Ashchepkov, I.V.; Vladykin, N.N.; Ntaflos, T.;. Kostrovitsky S.I.; Prokopiev S.A.; Downes H.; Smelov, A.P.; Agashev, A.M.; Logvinova, A.M.; Kuligin, S.S.; Tychkov, N.S.; Salikhov, R.F.; Stegnitsky, Yu.B.; Alymova, N.V.; Vavilov, M.A.; Minin, V.A.;

 doi:10.20944/preprints202108.0231.v1

Babushkina, S.A.; Ovchinnikov, Yu.I.; Karpenko, M.A.; Tolstov, A.V.; Shmarov, G.P. Layering of the lithospheric mantle beneath the Siberian Craton: Modeling using thermobarometry of mantle xenolith and xenocrysts. Tectonophysics **2014**, *634*, 55-75

27. Ashchepkov, I. V.; Alymova, N. V.; Logvinova, A. M.; Vladykin, N. V.; Kuligin, S. S.; Mityukhin, S. I.; Downes, H.; Stegnitsky, Yu. B.; Prokopiev, S.A.; Salikhov, R.F.; Palessky, V. S.; Khmel'nikova, O. S. Picroilmenites in Yakutian kimberlites: variations and genetic models. *Solid Earth* **2014**, *5*, 915–938,
28. Ashchepkov, I.V.; Vladykin, N.V.; Ntaflos, T.; Downes, H.; Mitchel, R.; Smelov, A.P.; Rotman,A.Ya.; Stegnitsky, Yu.; Smarov, G.P.; Makovchuk, I.V.; Nigmatulina, E.N.; Khmelnikova, O.S. Regularities of the mantle lithosphere structure and formation beneath Siberian craton in comparison with other cratons. *Gondwana Research* **2013**, *23*, 4–24.
29. Artemieva, I.M.; Mooney, W.D., Thermal structure and evolution of Precambrian lithosphere: A global study. *Journal of Geophysical Research* **2001**, *106*, 16387–16414.
30. Gladkochub, D.P.; Pisarevsky, S.A.; Donskaya, T.V.; Natapov, L.M.; Mazukabzov, A.M.; Stanevich, A.M.; Sklyarov, E.V. Siberian Craton and its evolution in terms of Rodinia hypothesis. Episodes **2006**, 29- 169–174.
31. Gladkochub, D.; Donskaya, T.; Mazukabzov, A.; Sklyarov, E.; Todt, W. Multistage magmatic and metamorphic evolution in the Southern Siberian Craton: Archean and Palaeoproterozoic zircon ages revealed by SHRIMP and TIMS. *Precambrian Research* **2005**, *136*, 353–368.
32. Kostrovitsky, S.I.; Morikiyo, T.; Serov, I.V.; Yakovlev, D.A.; Amirzhanov, A.A. 2007. Isotope-geochemical systematics of kimberlites and related rocks from the Siberian Platform. *Russian Geology and Geophysics* **2007**, *48/3*, 272-290,
33. Ashchepkov, I.V.; Logvinova, A.M.; Ntaflos, T.; Vladykin, N.V.; Downes, H., 2017. Alakit and Daldyn kimberlite fields, Siberia, Russia: Two types of mantle sub-terranes beneath central Yakutia? *Geoscience Frontiers* **2017**, *8*, 671–692.
34. Shatsky, V.S.; Zedgenizov, D.A.; Ragozin, A.L.; Kalinina, V.V. Diamondiferous subcontinental lithospheric mantle of the northeastern Siberian Craton: Evidence from mineral inclusions in alluvial diamonds. *Gondwana Research* **2015**, *28*, 106–120.
35. Griffin, W.L.; Batumike, J.M.; Greau, Y.; Pearson, N.J.; Shee S.R.; O'Reilly, S.Y. Emplacement ages and sources of kimberlites and related rocks in southern Africa: U–Pb ages and Sr–Nd isotopes of groundmass perovskite. *Contributions to Mineralogy and Petrology* **2004**, *168*, 1–13.
36. Tappe, S.; Smart, K.A.; Torsvik, T.H.; Massuyeau, M.; de Wit, M.C.J. Geodynamics of kimberlites on a cooling earth: Clues to plate tectonic evolution and deep volatile cycles. *Earth Planet. Sci. Lett.* **2018**, *484*, 1–14.
37. Field, M.; Stiefenhofer, J.; Robey, J.; Kurszlaukis, S. Kimberlite-hosted diamond deposits of southern Africa: A review. *Ore Geology Reviews* **2008**, *34*, 33–75.
38. Korolev, N.; Kopylova, M.; Gurney, J.J.; Moore, A.E. The origin of Type II diamonds as inferred from Cullinan mineral inclusions. *Mineralogy and Petrology* **2018**, *112*, 275–289.
39. Fitzgerald, C.E.; Hetman, C.M.; Lepine C.M.; Skelton, D.S.; McCandless, T.E. The internal geology and emplacement history of the Renard 2 kimberlite, Superior Province, Quebec, Canada. *Lithos* **2009**, *112S*, 513-528.
40. Hunt, L.C.; Stachel, T.; McCandless, T.E.; Armstrong, J.; Muehlenbachs, K. Diamonds and their mineral inclusions from the Renard kimberlites in Quebec. *Lithos* **2012**, *142–143*, 267–284.
41. Tappe, S.; Brand, N.B.; Stracke, A.; van Acken, D.; Liue, C.-Z.; Strauss, H.; Wu F.-Y.; Luguet A.; Mitchell, R.H. Plates or plumes in the origin of kimberlites: U/Pb perovskite and Sr-Nd-Hf-Os-C-O isotope constraints from the Superior craton (Canada). *Chemical Geology* **2017**, *455*, 57–83
42. Smit, K.V., Stachel, T., Stern, R.A. Diamonds in the Attawapiskat area of the Superior Craton (Canada): evidence for a major diamond-forming event younger than 1.1 Ga. *Contrib. Mineral. Petrol.* **2014**, *962,* 1–16.
43. Chalapathi Rao, N.V.; Lehmann, B.; Belyatsky B.; Warnslohd, M. The Late Cretaceous diamondiferous pyroclastic kimberlites from the Fort à la Corne (FALC) field, Saskatchewan craton, Canada: Petrology, geochemistry and genesis. *Gondwana Research* **2017**, *44*, 236–257
44. Scott Smith, B. H. Canadian kimberlites: Geological characteristics relevant to emplacement. Journal of *Volcanology and Geothermal Research* **2008**, *174*, 9–19.
45. Eggler, D.H.; McCallum, M.E.; Smith, C.B. Megacryst assemblages in kimberlite from northern Colorado and southern Wyoming: petrology, geothermometry –barometry and areal distribution. *In Kimberlites, Diatremes, and Diamonds:Their Geology, Petrology,and Geochemistry (eds. F.R.Boyd and H.O.A.Meyer). American Geophysical Union, Washington, DC* **1979**, *1*, 213–226.
46. Ashchepkov, I.V.; Downes, H.; Mitchell, R.; Vladykin, N.V.; Coopersmith, H.; Palessky, S.V. Wyoming Craton Mantle Lithosphere: Reconstructions Based on Xenocrysts from Sloan and Kelsey Lake Kimberlites. *G. Pearson* et al. *(eds.) Proceedings of 10th International Kimberlite Conference. - New Delhi: Springer India* **2013**, *1*, 13–27.
47. Kaminsky, F.V.; Zakharchenko O.D.; Griffin, W.L.; Der Channer D.M.; Khachatryan, G.K. Diamond from Guaniamo area, Venezuela. *The Canadian Mineralogist* **2000**, *38*, 1347–1370.
48. Schulze, D.J., Canil, D., Der Channer, C.D.M., Kaminsky F.V. Layered mantle structure beneath the western Guyana Shield, Venezuela: Evidence from diamonds and xenocrysts in Guaniamo kimberlites. *Geochimica Cosmochimica Acta,* **2006**, *70*, 192–205
49. Kaminsky, F.V., Sablukov, S.M., Belousova, E.A., Andreazza, P., Tremblay, M., Griffin, W.L. Kimberlitic sources of super-deep diamonds in the Juina area, Mato Grosso State, Brazil. *Lithos*, **2010**, *114*, 16–29.

50. Kaminsky, F.V., Zakharchenko, O., Davies, R., Griffin, W., Khachatryan-Blinova, G., Shiryaev, A. Superdeep diamonds from the Juina area, Mato Grosso State, Brazil. *Contrib. Mineral. Petrol.*, **2001**, *140*, 734– 753.
51. Meyer, H. O. A., Svisero, D.P. Mineral inclusions in Brazilian diamonds. *Physics and Chemistry of The Earth*, **1975**, *9*, 785–795.
52. Kaminsky, F.V., Sablukov, S.M.,.Sablukov, L.I,.Zakharchenko, O.D. The Fazenda Largo off-craton kimberlites of Piauí State, Brazil. *Journal of South American Earth Sciences*, **2009**, *28*, 288–303.
53. De Stefano A., Lefebvre N., Kopylova M. 2006. Enigmatic diamonds in Archean calc-alkaline lamprophyres of Wawa, southern Ontario, Canada. *Contrib. Mineral. Petrol.* **2006**, *151(2)*, 158-173
54. Stachel, T., Banas, A., Muehlenbachs, K., Kurszlaukis, S., Walker, E.C. 2006. Archean diamonds from Wawa (Canada): samples from deep cratonic roots predating cratonization of the Superior Province. *Contrib. Min. Petrol.*, **2006**, *151*, 737–750
55. Wyman, D.A., Kerrich, R., Polat, A. Assembly of Archean cratonic mantle lithosphere and crust: plume-arc interaction in the Abitibi–Wawa subduction–accretion complex, *Precambrian Res.*, **2002.**, *115*, 37–62.
56. Morris, T.F., Crabtree, D., Sage, R. P. Averill, S.A. Types, abundances and distribution of kimberlite indicator minerals in alluvial sediments, Wawa–Kinniwabi Lake area, Northeastern Ontario: implications for the presence of diamond-bearing kimberlite. *Journal of Geochemical Exploration*, **1998**. *63*, 217-235.
57. Aulbach, S., Creaser, R.A., Stachel, T., Heaman, L.M., Chinn, I. L., Kong, J. Diamond ages from Victor (Superior Craton): Intra-mantle cycling of volatiles (C, N, S) during supercontinent reorganization. *Earth and Planetary Science Letters*, **2018**, *490*, 77–87.
58. Stachel, T. Banas, A., Aulbach, S., Smit, K.V., Wescott, P., Chinn, I., Fisher, D., Kong, J. The Victor Mine (Superior Craton, Canada): Neoproterozoic lherzolitic diamonds from a thermally-modified cratonic root. *Mineral. Petrol.*, **2018**, *112*, 325–336.
59. Banas, A, Stachel, T, Muehlenbachs, K, McCandless, T.E. Diamonds from the Buffalo Head Hills, Alberta: Formation in a non-conventional setting. *Lithos*, **2007**, *93(1–2)*, 199–213.
60. Ivanova, O.A., Logvinova, A.M., Pokhilenko, N. P. Inclusions in diamonds from Snap Lake kimberlites (Slave Craton, Canada): Geochemical features of crystallization. *Doklady Earth Sciences*, **2017**, *474*, 490–493
61. Pokhilenko, N.P. Sobolev, N.V. Reutsky, V.N. Hall, A.E. Taylor, L. Crystalline inclusions and C isotope rations in diamonds from the Snap Lake/King Lake kimberlite dyke system: evidence of ultradeep and enriched lithospheric mantle. *Lithos*, **2004**, *77*, 57–67.
62. Pokhilenko, N.P., McDonald, J.A., Hall, A.E., Sobolev, N.V. Abnormally thick Cambrian lithosphere of the Southeast Slave Craton: evidence from crystalline inclusions in diamonds and pyrope compositions in Snap Lake kimberlites. *The Slave-Kaapvaal Workshop, Sep. 5-9, 2001, Merrickville, Ontario, Merrickvilli*, **2001**. 49-51
63. Pokhilenko, N.P., Sobolev, N.V., Cherny, S.D., Mityukhin, S.I., Yuanygin, Yu.T. Pyropes and chromites from the kimberlites of Nakyn field (Yakutia) and Snap Lake region (Slave craton, Canada): evidence of anomalous lithosphere structure. *Doklady Earth Sciences*, **2000**, *372 (3)*, 356-360.
64. Promprated, P., Taylor, L.A., Anand, M., Floss, C., Sobolev, N.V., Pokhilenko, N.P. Multiple-mineral inclusions in diamonds from the Snap Lake/King Lake kimberlite dike, Slave craton, Canada: a trace-element perspective. *Lithos.* **2004**, *77*, 69–81
65. Smart, K.A., Chacko, T., Stachel, T., Muehlenbachs, K., Stern, R.A., Heaman, L.M. Diamond growth from oxidized carbon sources beneath the Northern Slave Craton, Canada: A δ13C–N study of eclogite-hosted diamonds from the Jericho kimberlite. *Geochimica et Cosmochimica Acta*, **2011**, *75*, 6027–6047.
66. Smart, K.A., Heaman, L.M., Chacko, T., Simonetti, A, Kopylova, M., Mah, D, Daniels, D. The origin of high-MgO diamond eclogites from the Jericho Kimberlite, Canada. *Earth and Planetary Science Letters*, **2009**, *284*, 527–537.
67. De Stefano, A., Kopylova, M. G., Cartigny, P., Afanasiev, V. Diamonds and eclogites of the Jericho kimberlite (Northern Canada) *Contrib. Mineral. Petrol.*, **2009**, *158*, 295–315
68. Fedortchouk Y., Canil D., Carlson J.A. Oxygen Fugacity of Kimberlite Magmas and their Relationship to the Characteristics of Diamond Populations, Lac de Gras, N.W.T., Canada. *Extended Abstracts of the 8International Kimberlite Conference.* **2003**, *FLA_0098*.
69. Heaman, L., Creaser, R.A., Cookenboo, H., Chacko, T. Multi-stage modification of the Northern Slave mantle lithosphere: evidence from zircon- and diamond-bearing eclogite xenoliths entrained in Jericho kimberlite, Canada. *J. Petrol.* **2006**, *47*, 821–858.
70. Cartigny, P., Farquhar, J., Thomassot, E., Harris, J.W., Wing, B., Masterson, A. McKeegan, K., Stachel, T. A mantle origin for Paleoarchean peridotitic diamonds from the Panda kimberlite, Slave Craton: Evidence from 13C-, 15N- and 33,34S-stable isotope systematics. *Lithos*, **2009**, *112/2*, 852-864.
71. Donnelly, C.L., Stachel, T., Creighton, S., Muehlenbachs, K., Whiteford, S. Diamonds and their mineral inclusions from the A154 South pipe, Diavik Diamond Mine, Northwest territories, Canada. *Lithos*, **2007**, *98*, 160–176
72. Davies R.M., Griffin W.L, O'Reilly S.Y.,. Doyle B.J. Mineral inclusions and geochemical characteristics of microdiamonds from the DO27, A154, A21, A418, DO18, DD17 and Ranch Lake kimberlites at Lac de Gras, Slave Craton, Canada. *Lithos*, **2004**. *77*, 39– 55.
73. Tappert R, Stachel T, Harris JW, Brey GP (2005) Mineral inclusions in diamonds from the Panda kimberlite, Slave Province, Canada. *Eur. J. Mineral.*, **2005**, *17*, 423–440

74. Schulze, D.J., Coopersmith H.G., Harte B., Pizzolato L.-A. Mineral inclusions in diamonds from the Kelsey Lake Mine, Colorado, USA: Depleted Archean mantle beneath the Proterozoic Yavapai province. *Geochimica et Cosmochimica Acta,* **2008**, *72*, 1685–1695.
75. Otter, M.L., Gurney J.,J. Mineral Inclusions in Diamonds From the Sloan Diatremes, Colorado-Wyoming State Line Kimberlite District, North America. *Kimberlites and Related Rocks, Volume 2. Proceedings of the Fourth International Kimberlite Conference. Geological Society of Australia Special Publication 14, Perth, Australia,* **1986,** 1042–1053.
76. Wirth, R, Kaminsky, F, Matsyuk, S., Schreiber, A. Unusual micro- and nano-inclusions in diamonds from the Juina Area, Brazil. *Earth and Planetary Science Letters,* **2009**, *286*, 292–303.
77. Bulanova, G.P., Walter, M.J., Smith, C.B., Kohn, S.C., Armstrong, L.S., Blundy, J., Gobbo, L., Mineral inclusions in sublithospheric diamonds from Collier 4 kimberlite pipe, Juina, Brazil: subducted protoliths, carbonated melts and primary kimberlite magmatism. *Contributions to Mineralogy and Petrology,* **2010**, *160*, 489–510.
78. Kaminsky, F.V., Khachatryan, G.K., Andreazza, P., Araujo, D., Griffin, W.L. Superdeep diamonds from kimberlites in the Juina area, Mato Grosso State, Brazil. *Lithos,* **2009** *112 S2*, 833-842.
79. Tappert, R., Stachel, T., Harris, J.W., Muehlenbachs, K., Ludwig, T., Brey, G.P. Diamonds from Jagersfontein (South Africa): messengers from the sublithospheric mantle. *Contributions to Mineralogy and Petrology,* **2005** *150*, 505–522.
80. Deines, P., Harris, J.W., Gurney, J.J. The carbon isotopic composition and nitrogen content of lithospheric and asthenospheric diamonds from the Jagersfontein and Koffiefontein kimberlite, South Africa. *Geochimica et Cosmochimica Acta* **1999**, *55*, 2615–2625
81. Rickard, R.S., Harris, J.W., Gurney, J.J., Cardoso, P. Mineral inclusions in diamonds from Koffiefontein mine. *In: Ross, J., Jacques, A.L., Ferguson, J., Green, D.H., O'Reilly, S.Y., Danchin, R.V., Janse, A.J.A. (Eds.), Kimberlites and Related Rocks, Volume 2. Proceedings of the Fourth International Kimberlite Conference. Geological Society of Australia Special Publication 14, Perth, Australia,* **1989,** 1054–1062.
82. Appleyard, C.M., Bell, D.R., le Roex, A.P. Petrology and geochemistry of eclogite xenoliths from the Rietfontein kimberlite, Northern Cape, South Africa. *Contributions to Mineralogy and Petrology,* **2007** *154*, 309–333.
83. Smith, C.B., Gurney, J.J., Harris, J.W., Otter, M.L., Kirkley M.B., Jagoutz, E. Neodymium and strontium isotope systematics of eclogite and websterite paragenesis inclusions from single diamonds, Finsch and Kimberley Pool, RSA, *Geochimica et Cosmochimica Acta,* **1991** *55*, 2579–2590
84. Tsai, H.-M., Meyer, H.O.A., Moreau, J., Milledge, J. Mineral inclusions in diamond: Premier, Jagerfontein and Finsch kimberlites, South Africa, and Williams mine, Tansania. *Proceedings of the 2nd International Kimberlite Conference, American Geophysical Union,* **1979** *2*, 16-26.
85. Viljoen, K.S., Swash, P.M., Otter, M.L., Schulze, D.J. Lawless, P.J. Diamondiferous garnet harzburgites from the Finsch kimberlite, Northern Cape, South Africa. *Contrib. Mineral. Petrol.* **1992**, *110*, 133–138.
86. Viljoen, F., Dobbe, R., Harris, J., Smit, B. Trace element chemistry of mineral inclusions in eclogitic diamonds from the Premier (Cullinan) and Finsch kimberlites, South Africa: implications for the evolution of their mantle source. *Lithos,* **2010**, *118(1)*, 156-168.
87. Deines, P., Gurney, J.J and Harris, J.W., Associated chemical and carbon isotopic composition variations in diamonds from the Finsch and Premier kimberlites, South Africa. *Geochimica et Cosmochimica Acta,* **1984**, *48*, 325–342.
88. Gurney, J.J., Harris J.W., Rickard, R.S. Silicate and oxide inclusions in diamonds from the Finsch kimberlite pipe. *In: F.R. Boyd and H.O.A. Meyer, Editors, Kimberlites, Diatremes and Diamonds, their Geology, Petrology and Geochemistry, American Geophysical Union, Washington*, **1979**, 1–15.
89. Wilding, M.C., Harte, B. Fallick, A.E.., Harris, J.W. Inclusions, chemistry, carbon isotopes and nitrogen distribution in diamonds from the Bultfontein mine, South Africa, *Proc. of 5th Int. Kimb.Conf*., **1994**, *2*, p.116-126.
90. Phillips D., Harris, J.W., Viljoen, K.S. Mineral chemistry and thermobarometry of inclusions from De Beers Pool diamonds, Kimberley, South Africa. *Lithos,* **2004**, *77*, 155–179.
91. Jacob, D., Jagoutz, E. A. Diamond-graphite bearing eclogite xenolith from Roberts Victor (South Africa): implications for petrogenesis from Pb-, Nd-, and Sr isotopes. *In: Kimberlites, Related Rocksand Mantle Xenoliths (eds. H.O.A. Meyer and O.H. Leonardos) CPRM Spec.Publ. CPRM, Brasilia,* **1994**, *1*, 304–317
92. Deines, P., Harris, J.W., Gurney, J.J. Carbon isotopic composition, nitrogen content and inclusion composition of diamonds from the Roberts Victor Kimberlite, South Africa: evidence for 13 C depletion in the mantle. *Geochim. Cosmochim. Acta,* **1987**, *51*, 1227–1243.
93. Ishikawa, A., Pearson, D. G., Maruyama, S., Cartigny, P., Ketchum, R. A., Gurney, J. J. Compositional layering in a highly diamondiferous eclogite xenolith from the Roberts Victor kimberlite, South Africa and its implications for diamond genesis. *IX International Kimberlite Conf., Abst. No. 9IKC,* **2008**,*-A-00078.*
94. Riches, A.J.V. Ickert, R.B., Pearson, D.G., Stern, R.A., Jackson, S.E., Ishikawa, A., Kjarsgaard, B.A., Gurney, J.J. In situ oxygen-isotope, major-, and trace-element constraints on the metasomatic modification and crustal origin of a diamondiferous eclogite from Roberts Victor, Kaapvaal Craton. *Geochimica et Cosmochimica Acta,* **2016**.,*174*, 345-359.

95. Viljoen, K. S., Robinson, D.N., Swash, P. M., Griffin, W. L., Otter, M. L., Ryan, C. G., Win, T. T., Diamond- and graphite-bearing peridotite xenoliths 1161 from the Roberts Victor kimberlite, South Africa. *In: Meyer, H. O. A. and 1162 Leonardos, O. H. Eds.)5th International Kimberlite Conference.1163 Companhia de Pesquisa de Recursos Minerais, -Special Publication,* **1991**., 285– 303.
96. Viljoen, K. S., Perritt, S. H., Chinn, I. L. An unusual suite of eclogitic, websteritic and transitional websteritic-lherzolitic diamonds from the Voorspoed kimberlite in South Africa: Mineral inclusions and infrared characteristics. *Lithos,* **2018**, *320–321*, 416-434.
97. Karaevangelou, M., Kopylova, M., Loudon, P. Diamondiferous mantle beneath the Lace kimberlite in South Africa: evidence from mineral inclusions in diamonds Thesis for: Master of ScienceAdvisor: Maya Kopylova. *The University of British Columbia. (Vancouver)* **2019**. 163 p.
98. Aulbach, S.; Viljoen, K. S. 2015. Eclogite xenoliths from the Lace kimberlite, Kaapvaal craton: From convecting mantle source to palaeo-ocean floor and back. *Earth and Planetary Science Letters* **2015**, *431*, 274-286. doi:10.1016/j.epsl.2015.08.039
99. Daniels L., Gurney. J. 1998. Diamond Inclusions from the Dokolwayo Kimberlite, Swaziland. *In: J.J. Gurney, J.L., Gurney, M.D. Pascoe and S. H. Richardson (Editors), Proceedings of the VIIth International Kimberlite Conference, Red Roof Design, South Africa,***1998**, *2*, 134-142.
100. Gurney, J.J., Moore, R.O. 1986. Mineral Inclusions in Diamonds From the Monastery Kimberlite, South Africa. *Proceedings of the 4 th International Kimberlite Conference. At: Perth, Western Australia.* **1986**, *16*, 1029 -1041.
101. Gurney, J.J., Harris, J.W., Rickard R.S., Moore, R.O. Inclusions in Premier mine diamonds. South African *Journal of Geology,* **1985**, *88*, 301–310
102. Phillips, D., Onstott, T.C., Harris, J.W. 40Ar/39Ar laser-probe dating of diamond inclusions from the Premier kimberlite. *Nature,* **1989**, *340*, 460–462
103. McDade, P. and Harris, J.W. Syngenetic inclusion diamonds from Letseng-la-terai, Lesotho. *In: J.J. Gurney, J.L., Gurney, M.D. Pascoe and S. H. Richardson (Editors), Proceedings of the VIIth International Kimberlite Conference, Red Roof Design, South Africa,* **1999**, *2*, 557–565.
104. Phillips, D. Harris, J.W. Provenance studies from 40Ar/39Ar dating of mineral inclusions in diamonds: Methodological tests on the Orapa kimberlite, Botswana. Earth and Planetary Science Letters, 2008, 274, 169-178
105. Stachel, T., Viljoen, K.S., McDade, P., Harris, J.W. Diamondiferous lithospheric roots along the western margin of the Kalahari Craton the peridotitic inclusion suite in diamonds from Orapa and Jwaneng. *Contrib. Mineral. Petrol.*, **2004**, *147*, 32–47.
106. Ickert, R.B. Stachel, T., Stern, R.A., Harris, J.W. Diamond from recycled crustal carbon documented by coupled d18O–d13C measurements of diamonds and their inclusions.. *Earth and Planetary Science Letters.* **2013**, *364*, 85–97.
107. Gress, M,U. Michael U.Pearson, D.G., Chinn, I.L., Thomasso, E., Davies, G.R. Mesozoic to Paleoproterozoic diamond growth beneath Botswana recorded by Re-Os ages from individual eclogitic and websteritic inclusions. *Lithos,* **2021**, *388–389*, 106058.
108. Deines, P.; Harris, J.W. New insights into the occurrence of 13C-depleted carbon in the mantle from two closely associated kimberlites: Letlhakane and Orapa, Botswana. *Lithos* ***2004***, *77*, 125-142.
109. Honda, M., Phillip, D., Harris, J. W., Matsumoto, T. He, Ne and Ar in peridotitic and eclogitic paragenesis diamonds from the Jwaneng kimberlite, Botswana—Implications for mantle evolution and diamond formation ages. *Earth and Planetary Science Letters, 2011,* ***301***, 43–5
110. Richardson, S.H., Shirey, S.B., Harris J.W. Episodic diamond genesis at Jwaneng, Botswana, and implications for Kaapvaal craton evolution. *Lithos,* ***2004***, *177*, 43–154
111. Schrauder, M., Koeberl, C., Navon, O. Trace element analyses of fluid-bearing diamonds from Jwaneng, Botswana. *Geochim. Cosmochim. Acta,* **1996**, *60*, 4711–4724.
112. Viljoen, K.. An infrared investigation of inclusion-bearing diamonds from the Venetia kimberlite, Northern Province, South Africa: implications for diamonds from craton-margin settings. *Contributions to Mineralogy and Petrology*, **2002**, *144*, 98–108.
113. Richardson, S.H., Harris, J.W., Pöml, P.F. Antiquity of harzburgitic diamonds from the Venetia kimberlite, Limpopo Belt, Kaapvaal craton. *Geochimica et Cosmochimica Acta,* **2006**, *70*, 531.
114. Richardson, S.H., Pöml, P.F., Shirey, S.B., Harris, J.W. Age and origin of peridotitic diamonds from Venetia, Limpopo Belt, Kaapvaal–Zimbabwe craton. *Lithos,* **2009**,*.112S*, 785–792.
115. Kopylova, M.G., Gurney, J.J., Daniels, L.M. Mineral inclusions in diamonds from the River Ranch kimberlite, Zimbabwe. *Contributions to Mineralogy and Petrology,* **1997**, *129*, 366–384.
116. Smith, C.B. Sims K., Chimuk, L., Duffin, A., Beard, A.D., Townend, R. Kimberlite metasomatism at Murowa and Sese pipes, Zimbabwe. *Lithos,* **2004**, *76*, 219–232.
117. Aulbach, S., Höfer, H.E., Gerdes, A. High-Mg and Low-Mg Mantle Eclogites from Koidu (West African Craton) Linked by Neoproterozoic Ultramafic Melt Metasomatism of Subducted Archaean Plateau-like Oceanic Crust. *Journal of Petrology,* **2019**, *60*, 723–754.
118. Stachel,T., Harris, J. W. Syngenetic inclusions in diamond from the Birim field (Ghana) – a deep peridotitic profile with a history of depletion and re-enrichment. *Contributions to Mineralogy and Petrology,* **1997**, *127*, 336–352.
119. Harris J.W., Stachel T., Leost I., Brey G.P. 2004. Peridotitic diamonds from Namibia: constraints on the composition and evolution of their mantle source. *Lithos,* **2004**, *77*, 209–223

120. Kosman, C.W, Kopylova,.M.G., Stern, R.A., Hagadorn, J.W., Hurlbut, J.F. Cretaceous mantle of the Congo craton: Evidence from mineral and fluid inclusions in Kasai alluvial diamonds. *Lithos*, **2016**, *265*, 42–56
121. Nikitina, L.P., Korolev, N.M., Zinchenko, V.N. Felix. J.T. Eclogites from the upper mantle beneath the Kasai Craton (Western Africa): Petrography, whole-rock geochemistry and U - Pb zircon age. *Precambrian Research*, **2014**, *249*, 13–32.
122. Jaques, A.L., Hall, A.E., Sheraton, J.W., Smith, C.B., Sun, S.-S., Drew, R.M. Foudoulis, C., Ellingsen, K. Composition of crystalline inclusions and C-isotopic composition of Argyle and Ellendale diamonds. In: Ross, J., et al. (Eds.), Kimberlites and Related Rocks v. 2, Their Mantle/Crust Setting. *Geol. Soc. Of Australia Spec. Publ.*, **1989**, *14*, 966– 989.
123. Jaques, A.L., Luguet A., Smith, C.B., Pearson, D.G., Yaxley, G.M., Kobussen, A.F. Nature of the Mantle Beneath the Argyle AK1 Lamproite Pipe: Constraints from Mantle Xenoliths, Diamonds, and Lamproite Geochemistry. *Society of Economic Geologists, Special Publication*, **2018**, *20*, 119–143.
124. Jaques, A.L., O'Neill, H. St. C., Smith, C.B., Moon, J., Diamond-bearing peridotite xenoliths from the Argyle (AK1) pipe. *Contributions to Mineralogy and Petrology*, **1990**, *104*, 255 – 276.
125. Luguet, A., Jaques, A.L., Pearson, D.G., Smith. C.B., Bulanova, G.P., Roffey, S.L., Rayner, M.J., Lorand, J.-P. An integrated petrological, geochemical and Re–Os isotope study of peridotite xenoliths from the Argyle lamproite, Western Australia and implications for cratonic diamond occurrences. *Lithos*, **2009**, *112 S2;* 1096-1108.
126. Stachel, T., Harris, J.W., Hunt, L., Muehlenbachs, K., Kobussen, A.F., and Edinburgh. Ion Micro-Probe Facility, 2018, Argyle diamonds: How subduction along the Kimberley craton edge generated the world's biggest diamond deposit: *Society of Economic Geologists, Special Publication*, **2018**, *20*, 145–167
127. Timmerman, S. Honda, M., Zhang, X., Jaques, A.L, Bulanova, G., Smith, C.B., Burnham, A.D. Contrasting noble gas compositions of peridotitic and eclogitic monocrystalline diamonds from the Argyle lamproite. *Lithos*, **2019**, *344–345*, 193-206.
128. Sobolev, N.V., Kaminsky, F.V., Griffin, W.L., Yefimova, E.S., Win, T.T., Ryan, C.G., Botkunov, A.I. Mineral inclusions in diamonds from the Sputnik kimberlite pipe, Yakutia. *Lithos*, **1997**, *39*, 135–157.
129. Bulanova G.P., Pearson D.G., Hauri E.H., Griffin W.L. 2002. Carbon and nitrogen isotope systematics within a sector-growth diamond from the Mir kimberlite, Yakutia. *Chem. Geol.* **2002**, *188*, 105–123.
130. Bulanova, G.P., Wiggers de Vries, D.F., Pearson, D.G., Beard, A., Mikhail, S., Smelov, A.P., Davies, G.R. An eclogitic diamond from Mir pipe (Yakutia), recording two growth events from different isotopic sources. *Chemical Geology* **2014**, *381*, 40–54.
131. Ponomarenko, A.I. First find of a diamond bearing garnet-ilmenite peridotite in the Mir kimberlite pipe. *Doklady AN SSSR*, **1971**, *235*, 153– 156.
132. Sobolev, N.V., Botkunov, A.I., Lavrent'ev, Y.G., Usova, L.V. New data on the minerals associated with the diamonds in the "Mir" kimberlite pipe in Yakutia. *Sov. Geol. Geophys.*, **1976**, *17*, 1–10.
133. Sobolev, N.V. Logvinova, A.M. Zedgenizov, D.A. Seryotkin, Y.V. Yefimova, E.S., Floss, C., Taylor, L.A. Mineral inclusions in microdiamonds and macrodiamonds from kimberlites of Yakutia: a comparative study. *Lithos*, **2004**,. *77 (1-4)*, 225-242
134. Sobolev N.V., Logvinova A.M., Zedgenizov D.A., Yefimova E.S., Taylor L.A., Promprated P., Koptil V.I., Zinchuk N.N. Mineral Inclusions in Diamonds from Komsomolskaya and Krasnopresnenskaya Pipes, Yakutia: Evidence for Deep Lithospheric Heterogeneities in Siberian Craton. *8th International Kimberlite conference: Extended Abstracts*, **2003.** FLA_0141
135. Sobolev, N.V, Logvinova, A.M, Zedgenizov, D.A, Seryotkin, Y.V., Yefimova, E.S., Floss, C., Taylor, L.A., Mineral inclusions in microdiamonds and macrodiamonds from kimberlites of Yakutia: a comparative study. *Lithos*, **2004**, *77*, 225–242.
136. Logvinova, A.M., Wirth, R., Fedorova, E.N., Sobolev, N.V. Nanometric inclusions in cloudy Yakutian diamonds: compositon and paragenesis, *in: Crystallogenesis and Mineralogy. Russian Mineralogical Society*, **2007**, 173–187.
137. Logvinova, A.M. Taylor, L.A. Floss, C. Sobolev, N.V. Geochemistry of multiple diamond inclusions of harzburgitic garnets as examined in-situ. *International Geology Review*, **2005**, *47*. *(12)*, 1223-1233.
138. Sobolev, V.N., Taylor, L.A., Snyder, G.A., Sobolev, N.V. Diamondiferous eclogites from the Udachnaya pipe, Yakutia. *International Geology Review*, **1994**, *36 (1)*, 42-64.
139. Pokhilenko, L.N., 2006. Volatile composition and oxidation state of mantle xenoliths from Siberian kimberlites. PhD thesis, *United Institute of Geology Geophysics and Mineralogy, Novosibirsk.* **2006**, 225.
140. Pokhilenko, N.P., Sobolev N.V., Sobolev V.S. and Lavrentiev Y.G. Xenoliths of diamond bearing ilmenite-pyrope lherzolites from the kimberlite pipe Udachnaya (Yakutia).). *Doklady AN SSSR*, **1976**,.*231*, 438-442.
141. Bulanova, G.P., Griffin, W.L., Kaminsky, F.V., Davies, R., Ryan, C.G., Andrew, A., Spetsius, Z.V., Zahkarchenko, O.D. Diamonds from Zarnitsa and Dalnaya kimberlites (Yakutia): Their nature, growth history, and lithospheric mantle source *In: J.J. Gurney, J.L., Gurney, M.D. Pascoe and S. H. Richardson (Editors), Proceedings of the VIIth International Kimberlite Conference, Red Roof Design, South Africa*, **1998**, 21-24.
142. Reimers, L.F. Deep seated mineral associations of the kimberlites pipe Sytykanskaya (materials of the study of mantle rock and crystalline inclusions in diamonds). *Institute of Geology and Geophysics. Novosibirsk*. **1994**, 258 p.
143. Pernet-Fisher, J. F., Howarth, G.H., Liu, Y., Barry, P.H., Carmody, L., Valley, J.W., Bodnar, R.J., Spetsius, Z.V., Taylor L.A. Komsomolskaya diamondiferous eclogites: evidence for oceanic crustal protoliths. *Contributions to Mineralogy and Petrology*, **2014**, *167*,:981-999
144. Bulanova, G.P., Barashkov, Yu.P., Tal'nikova, S.B., Smelova, G.B. *Natural Diamond-genetic Aspects. Nauka, Novosibirsk,* **1993**. 176 pp. (in Russian

145. Riches, A. J.V., Liu, Y., Day J. M.D., Spetsius Z.V., Taylor L.A. Subducted oceanic crust as diamond hosts revealed by garnets of mantle xenoliths from. Nyurbinskaya, Siberia. *Lithos,* **2010**, *120*, 368–378.
146. Spetsius, Z.V. Taylor, L.A. Valley, J.W. Ivanov, A.S. Banzeruk, V.I.. Diamondiferous xenoliths from crustal subduction: Garnet oxygen isotopes from the Nyurbinskaya pipe, Yakutia. *European Journal of Mineralogy* **2008**, *20*, 375 – 385
147. Spetsius, Z.V., Ivanov, A.S.., Mityukhin, S. I. Diamondiferous xenoliths and megacrysts from the Nyurbinskaya kimberlite pipe (Nakynsky field, Yakutia). *Doklady Earth Sciences* **2006**, *409*, 779–783.
148. Sobolev N.V., Yefimova E.S., Reimers L.F., Zakharchenko O.D., Makhin A.I., Usova L.V. Arkhangelsk diamond inclusions. *6th Int. Kimberlite Conf., Novosibirsk, Ext. Abstr.,* **1995.** 558-560
149. Possoukhova, T.V., Kudryavtseva, G.P., Garanin, V.K. Diamonds and accompanying minerals from the Arkhangelsk kimberlite, Russia. *Rotterdam; Brookfield (Vt): A.A. Balkema, (1)* **1999**.. 667-670.
150. Rubanova, E.V., Palazhchenko, O.V., Garanin, V.K. Diamonds from the V. Grib pipe, Arkhangelsk kimberlite province, Russia. *Lithos,* **2009**, *112 S2*, 880–885.
151. Peltonen, P., Kinnunen, K.A., Huhma, H. Petrology of two diamondiferous eclogite xenoliths from the Lahtojoki kimberlite pipe, eastern Finland. *Lithos,* **2002**, *63*, 151–164
152. Sobolev, N.V., Logvinova, A.M., Tomilenko, A.A. Wirth, R., Bul'bak, T.A., Luk'yanova, L.I. Fedorova, E N., Reutsky, V.N., Efimova, E.S. Mineral and fluid inclusions in diamonds from the Urals placers, Russia: Evidence for solid molecular N2 and hydrocarbons in fluid inclusions. *Geochimica et Cosmochimica Acta,* **2019**, *266*, 197–219.
153. Laiginhas, F.A. Diamonds from the Ural Mountains: their characteristics and the mineralogy and geochemistry of their inclusions. *PhD Thesis University of Glasgow*. **2008**, 225 p.
154. Laiginhas, F., Pearson, D. G., Phillips, D., Burgess, R., Harris, J. W. Re–Os and 40Ar/39Ar isotope measurements of inclusions in alluvial diamonds from the Ural Mountains: Constraints on diamond genesis and eruption ages. *Lithos* **112**, *2009, S2*, 714-723
155. Chen, H, Qiu, Z. L, Lu, T.J, Stern, R.., Stachel, T., Sun, Yu., Zhang, J., Ke, J., Peng, S.Y., Qin, S.C. Variations in carbon isotopic composition in the subcontinental lithospheric mantle beneath the Yangtze and North China 1: Evidence from in-situ analysis of diamonds using SIMS. *Chin Sci Bull,* **2013**, *58*: 99-107.
156. Smith, C.B., Smith, Bulanova, G.P., Kohn, S.C., Milledge, H.J., Hall, A.E., Griffin, B.J. Nature and genesis of Kalimantan diamonds. *Lithos,* **2009**, *112(1)*, 822-832.
157. Smith, C.B., Bulanova, G.P., Kobussen, A.F., Burnham, A., Chapman, J.G., Davy, A.T., and Sinha, K.K. Diamonds from the Atri South pipe, Bunder lamproite field, India, and implications for the nature of the underlying mantle. *Society of Economic Geologists, Special Publication*, **2018**, *20*, 237–252.
158. Nimis, P., Taylor, W. Single clinopyroxene thermobarometry for garnet peridotites. Part I. Calibration and testing of a Cr-in-Cpx barometer and an enstatite-in-Cpx thermometer. *Contributions to Mineralogy and Petrology,* ***2000***, *139*, 541–554.
159. Nimis, P, Preston, R., Perritt, S.H., Chinn, I L. Diamond's depth distribution systematics. *Lithos,* **2020**, *376–377*, 105729
160. Korolev, N; Kopylova, M.; Gurney, John J.; Moore, A.E.; Davidson, J. The origin of Type II diamonds as inferred from Cullinan mineral inclusions. *Mineralogy and Petrology* **2018**, *112*, 275–289
161. Simakov, S.K., Taylor, L.A. Geobarometry for deep mantle eclogites: solubility of Ca-Tschermaks in clinopyroxene. *International Geological Review,* **2000**, *42*, 534–544.
162. Ryan C. G.; Griffin W. L.; Pearson N. J. Garnet geotherms: Pressure-temperature data from Cr-pyrope garnet xenocrysts in volcanic rocks. *J. Geophys. Res. B.* **1996**, *101*, 5611–5625.
163. Canil, D. The Ni-in-garnet geothermometer: calibration at natural abundances. *Contrib. Mineral. Petrol., 1999,* **136**, 240–246.
164. McGregor, I.D. The system MgO-SiO2-Al2O3: solubility of Al2O3 in enstatite for spinel and garnet peridotite compositions. *Am. Miner.,* **1974**, *59*, 110–119.*
165. Grutter H.S., Latti D. Menzies A.H. Cr-Saturation Arrays in Concentrate Garnet Compositions from Kimberlite and their Use in Mantle Barometry. *J. Petrol.,* **2006**, *47*, 4, 801–820
166. Kennedy, C.S., Kennedy, G.C. The equilibrium boundary between graphite and diamond. *J. Geophys. Res., 1976.* **81**, 2467-2470.
167. Day, H.W. A revised diamond-graphite transition curve. *American Mineralogist,* **2012**, *97*, 52–65.
168. Brey, G.P., Kohler, T. Geothermobarometry in four-phase lherzolites. II. New thermobarometers, and practical assessment of existing thermobarometers. *J. Petrol.,* **1990**, *31*, 1353-1378.
169. Nickel, K.G., Green, D.H. 1985. Empirical thermobarometry for garnet peridotites and nature of lithosphere, kimberlites and diamonds. *Earth. Planet. Sci. Lett., 1985,* **73**, *153*–170. Krogh, E.J. The garnet-clinopyroxene Fe-Mg geothermometer - a reinterpretation of existing experimental data. *Contrib. Mineral. Petrol.,* **1988**, *99*, 44–48.
170. O'Neill, H. St. C. and Wood B.J. An experimental study of Fe-Mg- partitioning between garnet and olivine and its calibration as a geothermometer. *Contributions to Mineralogy and Petrology, 1979,* **70**, 59–70.
171. Krogh, E.J. The garnet-clinopyroxene Fe-Mg geothermometer - a reinterpretation of existing experimental data. *Contrib. Mineral. Petrol.,* **1988**, *99*, 44–48.
172. Taylor, W.L., Kamperman, M., Hamilton, R. New thermometer and oxygen fugacity sensor calibration for ilmenite and Cr-spinel- bearing peridotite assemblage. *In: Gurney, J.J., Gurney, J.L., Pascoe, M.D., Richardson, S.H. (Eds.). 7th International Kimberlite Conference. In: Red Roof Design, Capetown*, **1998**, 986–988.

173. O'Neill, H.St.C., Wall, V.J. The olivine orthopyroxene-spinel oxygen geobarometer, the nickel precipitation curve, and the oxygen fugacity of the Earth's upper mantle. *Journal of Petrology*, **1987**, *8*, 1169–1191
174. Gudmundsson, G., Wood, B. 1995. Experimental tests of garnet peridotite oxygen barometry. *Contributions to Mineralogy and Petrology*, **1995**, *119*, 56–67.
175. Stagno, V, Frost, D.J., McCammon, C.A., Mohseni, H, Fei, Y. The oxygen fugacity at which graphite or diamond forms from carbonate-bearing melts in eclogitic rocks. *Contrib. Mineral. Petrol*., **2015**, 169, 16.
176. Pollack, H.N., Chapman, D.S., On the regional variation of heat flow, geotherms and lithospheric thickness. *Tectonophysics*, **1977**, *38*, 279- 296.
177. O'Reilly S.Y., Griffin W.L. A xenolith derived geotherm for southeastern Australia and it's geological implications. *Tectonophysics*. **1985**. *111*, 41-63.
178. Stagno, V. Frost, D.J. Carbon speciation in the asthenosphere: experimental measurements of the redox conditions at which carbonate - bearing melts coexist with graphite or diamond in peridotite assemblages. *Earth Planet. Sci. Lett.*, **2010**, *300*, 72-84.
179. Stagno, V., Ojwang, D.O., McCammon, C.A., Frost, D.J. The oxidation state of the mantle and the extraction of carbon from Earth's interior. *Nature*, **2013**, *493*, 84–88.
180. Afanasiev, V.P., Ashchepkov, I.V., Verzhak, V.V., O' Brien, H., Palessky, S.V. PT conditions and trace element variations of picroilmenites and pyropes from the Arkhangelsk region. *Journal of Asian Earth Sciences*, **2013**, *70–71*, 45-63.
181. Mikhailenko, D.S., Stagno, V., Korsakov, A.V., 2020. Redox state determination of eclogite xenoliths from Udachnaya kimberlite pipe (Siberian craton), with some implications for the graphite/diamond formation. *Contrib. Mineral. Petrol.* 175, **2020**, *107*.
182. Jacob, D.; Jagoutz, E.; Lowry, D.; Mattey, D.; Kudrjavtseva, G. Diamondiferous eclogites from Siberia: Remnants of Archean oceanic crust. *Geochim. Cosmochim. Acta*, **1994**, *58*, 5191–5207.
183. Sobolev, N.V.; Taylor, L.A.; Zuev, V.M.; Bezborodov, S.M.; Snyder, G.A.; Sobolev, V.N.; Yefimova, E.S. The specific features of eclogitic paragenesis of diamonds from Mir and Udachnaya kimberlite pipes (Yakutia). *Russ. Geol. Geophys.* **1998**, *39*, 1653–1663.
184. Shatsky, V.S.; Ragozin, A.L.; Zedgenizov, D.A.; Mityukhin, S.I. Evidence for multistage evolution in a xenolith of diamond-bearing eclogite from the Udachnaya kimberlite pipe. *Lithos* **2008**, *105*, 289–300.
185. Sobolev, V.N.; Taylor, L.A.; Snyder, G.A.; Sobolev, N.V. Diamondiferous eclogites from the Udachnaya kimberlite pipe, Yakutia. *Int. Geol. Rev*. **1994**, *36*, 42–64.
186. Snyder, G.A., Jerde, E.A., Taylor, L.A., Halliday, A.N., Sobolev, V.N., Sobolev, N.V., 1993. Nd and Sr isotopes from diamondiferous eclogites, Udachnaya kimberlite pipe, Yakutia, Siberia: evidence of differentiation in the early Earth? Earth and Planetary Science Letters 118, 91–100.
187. Misra, K.C.; Anand, M.; Taylor, L.A.; Sobolev, N.V. Multi-stage metasomatism of diamondiferous eclogite xenoliths from the Udachnaya kimberlite pipe, Yakutia, Siberia. *Contrib. Mineral. Petrol.* **2004**, *146*, 696–714.
188. Pokhilenko, N.P., Sobolev, N.V., Kuligin, S.S., Shimizu, N. Peculiarities of distribution of pyroxenite paragenesis garnets in Yakutian kimberlites and some aspects of the evolution of the Siberian craton lithospheric mantle. *Proceedings of the VII International Kimberlite Conference. The P.H. Nixon volume.* **1999**. p. 690-707
189. McCammon, C.A., Griffin, W.L., Shee, S.R., O'Neill, H.S.C. Oxidation during metasomatism in ultramafic xenoliths from the Wesselton kimberlite, South Africa: implications for the survival of diamond. *Contrib. Mineral. Petrol.*, **2001**, *141*, 287–29
190. Stachel, T., Harris, J.W., Brey, G.P. Rare and unusual mineral inclusions in diamonds from Mwadui, Tanzania. *Contributions to Mineralogy and Petrology*, ***2004***, *132*, 34–47.
191. Motsamai, T.; Harris, J.W.; Stachel, T.; Graham Pearson, D.G.; Armstrong, J. Mineral inclusions in diamonds from Karowe Mine, Botswana: super-deep sources for super-sized diamonds? *Mineralogy and Petrology*, **2018**, *112*, 169–180.
192. Nestola, F., Zafro, G., Mazzucchelli, M.L., Nimis,P., Andreozzi, G.B., Periotto, B., Princivalle, F., Lenaz, D., Secco, L., Pasqualetto, L., Logvinova, A.M., Sobolev, N.V., Lorenzetti, A., Harris, J.W. Diamond-inclusion system recording old deep lithosphere conditions at Udachnaya (Siberia). *Nature*, **2019**, *12586.*
193. De Hoog, J. C. M., Stachel, T., Harris, J. W. Trace-element geochemistry of diamond-hosted olivine inclusions from the Akwatia Mine, West African Craton: implications for diamond paragenesis and geothermobarometry. *Contributions to Mineralogy and Petrology*, **2019**, *174*, 100
194. Weiss, Y., Navon, O., Goldstein, S.L., Harris, J.W. Inclusions in diamonds constrain thermo-chemical conditions during Mesozoic metasomatism of the Kaapvaal cratonic mantle. *Earth and Planetary Science Letters*, **2018**, *491*, 134–147.
195. Timmerman, S.; Krebs, M.Y.; Pearson, D.G.; Honda, M. Diamond-forming media through time – Trace element and noble gas systematics of diamonds formed over 3 billion years of Earth's history. *Geochimica et Cosmochimica Acta* **2019**, *257* , 266-283
196. Malkovets, V.G., Griffin, W.L., O'Reilly, S.Y., Wood, B.J. Diamond, subcalcic garnet, and mantle metasomatism: Kimberlite sampling patterns define the link. *Geology*, **2007**, *35*, 339–342.
197. Simakov, S.K. On the origin of large type IIa gem diamonds. *Ore Geology Reviews*, *2018*, **102**, 195-203
198. Kopylova, M., Navon, O., Dubrovinsky, L., Khachatryan, G. Carbonatitic mineralogy of natural diamond-forming fluids. *Earth and Planetary Science Letters*, **2010**, *291*, 126–137
199. Aulbach, S., Stachel, T., Heaman, L.M., Carlson, J.A. Microxenoliths from the Slave craton: archives of diamond formation along fluid conduits. *Lithos*, **2011**, *126*, 419-434.

200. Palot, M., Pearson, D.G., Stern, R.A., Stachel, T., Harris, J.W. Isotopic constraints on the nature and circulation of deep mantle C–H–O–N fluids: Carbon and nitrogen systematics within ultra-deep diamonds from Kankan (Guinea). *Geochimica et Cosmochimica Acta*, **2014**, *139*, 26–46.
201. Krebs, M.Y., Pearson, D.G., Stachel, T., Laiginhas, F., Woodland C., Chinn, I., Kong, J.A. Common parentage-low abundance trace element data of gem diamonds reveals similar fluids to fibrous diamonds. *Lithos*, ***2019***, *324*–325, 356-370.
202. Liu, Y., Taylor, L. A., Sarbadhikari, A.B., Valley, J.W., Ushikubo, T, Spicuzza, M.J., Kita, N., Ketcham, R.A., Carlson, W. Shatsky, V., Sobolev N.V. Metasomatic origin of diamonds in the world's largest diamondiferous eclogites. *Lithos*, **2009**, *112S*, 1014–1024
203. Pal'yanov, Y.N., Sokol, A. G., Borzdov, M., Khokhryakov, A.F. Fluid-bearing alkaline carbonate melts as the medium for the formation of diamonds in the Earth's mantle: an experimental study. *Lithos*, **2002**, *60*, 145–159.
204. Palyanov, Y.N., Sokol, A.G., Borzdov, Y.M., Khokhryakov, A.F., Sobolev, N.V. Diamond formation through carbonate-silicate interaction. *American Mineralogist, 2002,* **87**, 1009–1013.
205. Moore, A. E. and Lock, N. P.: The origin of mantle-derived megacrysts and sheared peridotites - evidence from kimberlites in the northern Lesotho - Orange Free State (South Africa) and Botswana pipe clusters. *South Africa Journal of Geology*, **2001**, *104(1)*, 23-38.
206. Moore, A. Type II diamonds: Flamboyant Megacrysts? *South African Journal of Geology*, **2009**, *112(1)*, 23-38
207. Rege, S., Griffin, W.L., Kurat, G., Jackson, S.E., Pearson, N.J., O'Reilly S.Y. Trace-element geochemistry of diamondite: Crystallisation of diamond from kimberlite–carbonatite melts. *Lithos*, **2008**, *106*, 39–54.
208. Schmitt, A.K., Zack, T., Kooijm, E., Logvinova, A.M., Sobolev, N.V. 2019. U–Pb ages of rare rutile inclusions in diamond indicate entrapment synchronous with kimberlite formation. *Lithos*, **2019**, *350–351*, 105251
209. Karato, S. Rheology of the Earth's mantle: A historical review. *Gondwana Research*, **2010**, *18*, 17–45.
210. Wang, W. Formation of diamond with mineral inclusions of "mixed'' eclogitic and peridotitic paragenesis. *Earth Planet Sci Lett.*, **1998**, *160*, 831–843
211. Shirey, S.B., Harris, J.W., Richardson, S.H., Fouch, M., James, D.E., Cartigny, P., Deines, P., Viljoen, F. Regional patterns in the paragenesis and age of inclusions in diamond, diamond composition, and the lithospheric seismic structure of Southern Africa. *Lithos*, **2003**, *71*, 243–258
212. Afanasyev, V.P., Agashev, A.M., Orihashi, Y., Pokhilenko, N.P., Sobolev, N.V. Paleozoic U–Pb Age of Rutile Inclusions in Diamonds of the V–VII Variety from Placers of the Northeast Siberian Platform. *Doklady Earth Sciences*, **2009**, *428*, 1151–1155.
213. Pokhilenko N.P., Pearson D.G., Boyd F.R., Sobolev N.V. Megacrystalline dunites: sources of Siberian diamonds. *Carnegie Inst. Wash..Yearb.* **1991**, *90*, 11–18.
214. Stachel, T., Viljoen, K.S., Brey, G. and Harris, J.W. Metasomatic processes in lherzolitic and harzburgitic domains of diamondiferous lithospheric mantle: REE in garnets from xenoliths and inclusions in diamonds. *Earth and Planetary Science Letters*, **1998**, *159*, 1–12.
215. Wang, W., Sueno, S, Takahashi, E., Yurimoto, H., Gasparik, T. Enrichment processes at the base of the Archean lithospheric mantle: observations from trace element characteristics of pyropic garnet inclusions in diamonds. *Contributions to Mineralogy and Petrology*, **2000**, *139*, 720–733.
216. Ionov, D.A., Liu, Z., Li, J., Golovin A.V., Korsakov, A.V., Xua, Y. The age and origin of cratonic lithospheric mantle: Archean dunites vs. Paleoproterozoic harzburgites from the Udachnaya kimberlite, Siberian craton. *Geochimica et Cosmochimica Acta,* **2020**, *281*, 67–90.
217. Wyman, D.A., Ayer, J.A. Conceição, R.V., Sage, R.P. Mantle processes in an Archean orogen: Evidence from 2.67 Ga diamond-bearing lamprophyres and xenoliths. *Lithos*, **2006**, *89*, 300–328.
218. Smit, K.V., Shirey, S.B. Wang, W. Type Ib diamond formation and preservation in the West African lithospheric mantle: Re–Os age constraints from sulphide inclusions in Zimmi diamonds. *Precambrian Research*, **2016**, *286*, 152–166
219. Shu,Q., Brey, G.P. Ancient mantle metasomatism recorded in subcalcic garnet xenocrysts: Temporal links between mantle metasomatism, diamond growth and crustal tectonomagmatism. *Earth and Planetary Science Letters,* **2015**, *418*, 27–39.
220. Klein-Ben David, O., Pearsona, D.G. Origins of subcalcic garnets and their relation to diamond forming fluids—Case studies from Ekati (NWT-Canada) and Murowa (Zimbabwe). *Geochimica et Cosmochimica Acta*, **2009,** *73*, 837–855
221. Grütter, H.S., Gurney, J.J., Menzies, A.H., Wintera, F. An updated classification scheme for mantle-derived garnet, for use by diamond explorers. *Lithos*, **2004**, *77*, 841–857.
222. Gurney, J.J. A correlation between garnets and diamonds. In: Glover, J.E., Harris, P.G. (Eds.), Kimberlite Occurrence and Origin: A basis for conceptual models in exploration. *Geol. Dept. and Univ. Ext., Univ. of WA Publ.*, **1984**, *8*, 143–166
223. Dludla,S., le Roex, A.P., Gurney, J.J. Eclogite xenoliths from the Premier kimberlite, South Africa: geochemical evidence for a subduction origin. *South African Journal of Geology*, **2006**, *109*, 353–368.
224. Spetsius, Z.V. Two generation of diamonds in the eclogite xenoliths. *Proc. 7th Int. Kimberlite Conf., Cape Town*, **1999**. 823–828
225. Haggerty, S.E. 1999. A diamond trilogy: superplumes, super continents, and supernovae. *Science*, **1999**, *285*, 851–860.
226. Jacob, D.E., Foley, S.F. Evidence for Archean ocean crust with low high field strength element signature from diamondiferous eclogite xenoliths. *Lithos*, **1999**, *48*, 317–336.
227. Richardson, S.H. Latter-day origin of diamonds of eclogitic paragenesis. *Nature*, **1986**, *322*, 623–626.

 doi:10.20944/preprints202108.0231.v1

228. Richardson, S.H., Shirey, S.B., Harris, J. W., Carlson, R.W. 2001. Archean subduction recorded by Re–Os isotopes in eclogitic sulfide inclusions in Kimberley diamonds. *Earth Planet. Sci. Lett.*, **1986**, *191*, 257–266.
229. Ernst, R.E., Davies, D.R., Jowitt, S.M., Campbell, I.H. When do mantle plumes destroy diamonds? *Earth and Planetary Science Letters*, **2018**, *502*, 244–252..
230. Hasterok, D. & Chapman, D. S. Heat production and geotherms for the continental lithosphere. *Earth Planet. Sci. Lett.*, **2011,** *307*, 59–70.
231. Stagno, V.; Stopponi, V.; Kono, Y.; D'Arco, A.; Lupi, S.; Romano, C.; Poe, B.T.; Foustoukos, D.I.; Scarlato, P.; Manning, C.E. The Viscosity and Atomic Structure of Volatile-Bearing Melilititic Melts at High Pressure and Temperature and the Transport of Deep Carbon. *Minerals* **2020**, *10*, 267.
232. Ashchepkov I.V., Vladykin N.V., Ivanov A., Babushkina S., Vavilov M., Medvedev N. (2021) Problems of Mantle Structure and Compositions of Various Terranes of Siberian Craton. *In: Vladykin N. (eds) Alkaline Rocks, Kimberlites and Carbonatites: Geochemistry and Genesis. Springer Proceedings in Earth and Environmental Sciences. Springer, Cham.* 2021, 11-48. https://doi.org/10.1007/978-3-030-69670-2_2
233. Aulbach, S.; Stagno, V. Evidence for a reducing Archean ambient mantle and its effects on the carbon cycle. Geology 2016, 44, 751–754.
234. Tappert, R., Stachel, T., Harris, J.W., Muehlenbachs, K., T., Brey, G.P. Placer Diamonds from Brazil: Indicators of the Composition of the Earth's Mantle and the Distance to Their Kimberlitic Sources. *Economic Geology*, **2006**,*101*, 453–470
235. Czas, J., Pearson, D. G., Stachel, T., Kjarsgaard, B.A., Read, G.H. Palaeoproterozoic diamond-bearing lithospheric mantle root beneath the Archean Sask Craton, Canada. *Lithos*, **2020**, *356–357*, 105301
236. Sobolev, N. V., Pokhilenko, N. V., Efimova, E.S. Xenoliths of diamond bearing peridotites in kimberlites and problem of the diamond origin. *Russian Geology and Geophysics*, **1984**, *25/12*, 63-80.
237. Taylor, L. A., Anand, M. Diamonds: time capsules from the Siberian Mantle. *Chemie der Erde*, **2004**, *64*, 1–74
238. Taylor, L.A., Anand, M., Promprated, P., Floss, C., Sobolev, N.V. The significance of mineral inclusions in large diamonds from Yakutia, Russia. *American Mineralogist*, **2003**, *88*, 912–920
239. Taylor, L.A., Snyder, G.A., Crozaz, G., Sobolev, V.N., Yefimova, E.S., Sobolev, N.V. Eclogitic inclusions in diamonds: Evidence of complex mantle processes over time. *Earth Planet. Sci. Lett.*, **1996**, *142*, 535–551.
240. Spetsius, Z.V., Belousova, E.A., Griffin W. L., O'Reilly S.Y., Pearson N.J. Archean sulfide inclusions in Paleozoic zircon megacrysts from the Mir kimberlite, Yakutia: implications for the dating of diamonds. Earth *Planet Sci Letters..*, **2002**, *199*, 111–126.
241. Pearson, D.G., Canil, D., Shirey, S.B. Mantle samples included in volcanic rocks: xenoliths and diamonds. *In: Turekian, K. K., Holland, H. D. (eds) Treatise on Geochemistry, Volume 2: The Mantle and Core, Amsterdam: Elsevier.* **2003**, 171